Atomic Energy of Canada Limited

TREFOIL BUNDLES OF NPD 7-ELEMENT SIZE FUEL IRRADIATED TO 9100 MWd/tonne U

CRFD-1179

by

A.S. BAIN, J. CHRISTIE and A.R. DANIEL

Chalk River, Ontario

January, 1964

AECL-1895

TREFOIL BUNDLES OF NPD 7-ELEMENT SIZE FUEL IRRADIATED TO 9100 MWd/tonne U

by

A.S. Bain, J. Christie and A.R. Daniel

Abstract

NPD prototype elements (1 in. OD, 19 in. long) were assembled into trefoil bundles and irradiated in the X-5 pressurized-water loop of NRX. The first tests were for only a few weeks but showed that elements made by sheathing UO_2 pellets in Zircaloy-2 behaved well under irradiation; later similar elements were irradiated for 18000 hours to a burn-up of 9100 MWd/tonne U at $\int kd\theta = 40$ W/cm. The dimensional stability of all the elements was good. Only those subjected to long irradiation showed progressive diametral increases, and these were attributed to relocation of the UO_2 during interim inspections. Length measurements demonstrated that pellet end-dishing is effective in controlling axial expansion, but that for a given depth of dishing the amount of expansion depends on the shoulder width. The extent of grain growth in the UO_2 was compatible with previously reported results when the duration of irradiation, density of the fuel, and variations in growth characteristics of the different batches of UO_2 are considered. The elements taken to high irradiation released up to 135 ml of fission-product gases, which is 2% of the amount formed.

The transverse tensile strength of ring samples from the Zircaloy-2 sheaths increased from 75000 to 95000 lb/in^2 at room temperature, but the ductility dropped. The completely brittle fracture of some rings was due to ZrH_2 precipitation. The failure of one element was caused by increased stress due to a higher heat rating, combined with low ductility of the Zircaloy-2 resulting from radiation damage and with precipitation of ZrH_2 because of a lower coolant temperature. The fission-product release from the split was not excessive, and the element was easily withdrawn from the loop after operating at full power for four days from the time of the failure.

AECL-1895

Chalk River, Ontario
January 1964

1. INTRODUCTION

The fuel for the heavy-water-moderated Canadian power reactors is stoichiometric natural uranium oxide sheathed in Zircaloy-2. For the NPD+ reactor the fuel was originally to consist of 1 in. diameter, 19 in. long elements assembled into 7-element bundles. Later the core loading was changed so that only the outer rings contained the 7-element bundles, while the central regions contained bundles consisting of 19 elements, each element being 0.6 in. outer diameter and 19 in. long. In 1958, under the joint sponsorship of Atomic Energy of Canada Limited, Chalk River, Ontario, and the Civilian Atomic Power Department of Canadian General Electric, Peterborough, Ontario, a series of tests was initiated to determine the irradiation behaviour of the 7-element size fuel when exposed to a burnup up to 10000MWd/te of U. With the loop facilities available at that time it was not possible to irradiate a complete bundle. Therefore three elements were assembled into a trefoil arrangement and inserted into the X-5 (formerly CR-V) loop located in the central thimble of the NRX reactor. Testing of complete 7-element and 19-element bundles started when the E-20 loop of the NRU reactor became available.

The first trefoil irradiation was designated CR-V-k. As originally planned, CR-V-k was to test a prototype fuel geometry which called for a nominal one inch outer diameter and 0.025 in. wall thickness Zircaloy-2 sheath. The diametral clearance between the fuel and sheath was 0.012 in. and the axial clearance was between 0.25 and 0.6 in. Nine elements of this type were fabricated but during autoclaving at 750°F and 1500 lb/in^2 the sheath collapsed onto the pellets and into the axial gap. Further testing showed that 0.006 in. diametral clearance was the largest which could be used without plastic deformation of the sheath at operating conditions. The internal voidage necessary to accommodate thermal expansion of the UO_2 was provided by grinding dishes in the ends of the sintered pellets.

The second, third and fourth tests were to include design changes which were indicated by the results of the previous tests and from concurrent irradiations in other loops. However, because of lack of time, the second trefoil irradiation had to be designed before the CR-V-k results were available. It was therefore decided that one of the bundles should incorporate thicker sheaths in case

---

+ Nuclear Power Demonstration reactor now operating at ROLPHTON, Ontario.

the 0.025 in. thick sheaths of the CR-V-k tests proved unsuitable.

2. OBJECTIVES

The designation of the four tests which comprised the trefoil irradiations, plus the major objectives and variations in the fabrication parameters were given in the separate proposals (1) and are summarized in Table 1.

3. FABRICATION

The uranium dioxide fuel was prepared by AECL from ammonium diuranate precipitate. Details of the preparation were reported in the fabrication reports for the various charges (1). A summary is given in Table 2. Procurement of the Zircaloy-2 components, welding of the individual elements in an argon atmosphere, and assembly of the bundles was done by CAPD, Peterborough. The inter-element spacing in the trefoil bundles was maintained with 0.050 in. diameter wire wrap. In the first tests the wire was mechanically attached to the end caps of the elements; in bundle TT the acceptability of spot-welded wire wrap was tested. Complete details of the fabrication have been reported by CGE (1). During autoclaving of the CR-V-n test the controller failed and the autoclave was opened. All elements were extensively covered with white corrosion products which were removed with vapour blasting. Elements were pickled then re-autoclaved in steam at 750°F, 800 lb/in^2 for 18 hours. Excessive corrosion in the first test was due to welding slag and a monel shelf inside the autoclave.

In Table 3 the dimensions of each element are given. In Figure 1 an assembled bundle, two individual elements, a spacer rod and a capillary tube, to hold cobalt wire monitors are shown.

4. IRRADIATION HISTORY

The dates of insertion and final removal of the four tests are given in Table 4. In accordance with an agreement between AECL and Bettis Atomic Power Laboratories, Pittsburgh, Penn., the X-5 loop was shared during part of the irradiation period; AECL occupied the top half and BAPL the bottom half of the loop. The positions of each AECL bundle during the four tests are given on Figure 2. Details of each irradiation are summarized below.

4.1 Test CR-V-k

The uranium oxide was enriched to nominally 2.3 wt% U-235 in total U. With the reactor operating

at full power and an extrapolated flux height of 320 cm it was predicted that the maximum surface heat flux would be 74.4 W/cm^2, resulting in a value of $K(T_s,T_o)^+$ = 47 W/cm. After fabrication of the elements the heat fluxes were recalculated, based on what was considered a better method of homogenizing the coolant and the fuel bundle. The revised figures were 125 W/cm^2 and $K(T_s,T_o)$ = 78.5 W/cm. These values were well above the 10% overload limit allowed for the test; therefore the safety of the experiment was in doubt. A specific schedule of reactor operation was detailed to ensure that the power was raised slowly, and that the heat ratings of the elements did not reach exceptionally high levels. Details of the actual operation are given in Table 5.

4.2 Test CR-V-m

To prevent burnout of the BAPL fuel which was inserted in the lower half of the loop it was necessary to raise the loop pressure 200 lb/in.^{2} above the proposed NPD operating pressure of 1000 lb/in.^{2}. The charge was installed and the loop pressure tested to 1800 lb/in.^{2} at room temperature, then the coolant was degassed and brought to operating temperature of 260°C. The irradiation proceeded without incident and the fuel was removed on schedule.

4.3 Test CR-V-n

The loop was pressure tested and operated in a manner similar to that for the CR-V-m test. The irradiation proceeded until November 16, 1959 when both bundles were removed. After a preliminary examination it was decided that bundle P would be re-inserted in the loop along with the two bundles of the X-5-o* tests which had been installed on December 7, 1959. Bundle K-J of test CR-V-n was destructively examined.

4.4 Test X-5-o

After pressure testing of the loop the reactor was started on December 7, 1959, with the two bundles from the X-5-o test, (one a trefoil bundle TT, and the other an eight-element bundle, OC). On December 14, 1959, the reactor was shut down and bundle P from the CR-V-n

---

+ $K(T_s,T_o) = \int_{T_s}^{T_o} k\,d\theta$ where k is thermal conductivity of UO_2 at temperature θ. Subscripts s,g and o are applied to the limits of integration to represent the temperature of the surface, position of discernible grain growth and center respectively.

* The CR-V loop was renamed the X-5 loop at this time.

test inserted in the high flux position in the loop, as illustrated in the loading diagram (Figure 2). On December 22, 1959 high activity in the loop necessitated removal of all the fuel. Examination showed that a BAPL element was defective and that the three AECL bundles were intact. The irradiation of these bundles continued from January 22, 1960 to March 21, 1960, when bundle P was removed for examination. Since there was no appreciable change from previous examinations the bundle was returned for further irradiation. The irradiation of the three bundles continued until August 23, 1960, when the octafoil bundle OC was removed and placed in storage, and will not be discussed further in this report. Bundles TT and P were re-inserted and were irradiated together until July 24, 1961. During this period they were examined four times, then re-inserted, always at the same level in the loop. From June 28, 1961 to July 24, 1961 only bundle TT was in the loop. Bundle P was examined and the lower end plate was found to be broken. Extra end plates were attached, both at the broken and the intact end. A spacer rod was removed and sectioned for hydrogen analyses. A new spacer was installed and the bundle returned to the reactor at the position of high flux on July 25, 1961. The irradiation of the two bundles proceeded as before until September 18, 1961. At that time the bundles were relocated so that bundle P was just below, and bundle TT just above the flux centerline, as shown in the loading diagram (Figure 2).

At 0400 hours on September 29, 1961, the reactor was started with the X-5 loop coolant at 190°C after a one day shutdown, which was not connected with X-5 loop. The reactor tripped at 1600 hours, then was brought back to power at 1800 hours. At 1900 hours, when the reactor was at full power with a moderator level 258 cm above the calandria bottom, activity was detected in the loop coolant. The reactor was shut down at 1530 hours on October 2, 1961, and the bundles removed. Examination revealed a split in element TT-4, whereas the other elements of TT and all elements of bundle P appeared sound. The defective element was removed from the bundle and element TL-2 put in its place. Both bundles were inserted as part of composite charges in the X-5 loop with bundle P at the high flux position and bundle TT directly below, as illustrated in Figure 2. The irradiation was terminated on May 22, 1962. A more detailed list of the various loadings of the X-5-o test is given in Table 6.

5. HEAT RATINGS

The power output of each bundle was determined by Hart and Durham from the calorimetric output of the loop, and by chemical analyses of the U-235 depletion, where available, or the plutomium:uranium ratio. A comparison between the output of the bundles from

different tests was made by taking into account the difference in weight of uranium, U-235 enrichment, relative power output of loop (f factor)+, and fraction of neutron flux at the position of the various bundles. No allowance was made for U-235 burn-out in bundles P and TT. In general, good agreement was obtained, giving confidence in the power outputs obtained from calorimetric measurements alone. In Table 7, the positions of each bundle and the percentage of the thermal neutron flux are given. In Tables 8 and 9 the output of each element, the heat output per unit length, and values of $K(T_s,T_o)$ are presented.

6. POST-IRRADIATION EXAMINATION

Fuel from the CR-V-k and CR-V-m tests, and bundle K-J from the CR-V-n test had only one loading; after removal from the reactor they were transferred for post-irradiation examination. Bundles P and TT from test X-5-o had several loadings; between some loadings the bundles received an interim inspection for surface defects and dimensional changes. The final examination of all bundles consisted of visual inspection, photography, mensuration, puncture for fission-product gas release, and cross-sectioning at intervals along the length. From selected elements pieces of fuel and sheathing were metallographically examined. Samples were removed for hydrogen analyses of the sheath and complete pellets were extracted for chemical burn-up. Rings of sheathing were cut from each element of bundles TT and P for tensile testing.

6.1 Visual Examinations

6.1.1 Tests CR-V-k, CR-V-m and CR-V-n

The bundles from the above tests were in good condition. No bundle deformation or specimen bowing was noted, and no white corrosion products were observed. The end plates were straight, and the wire wrap was unchanged.

6.1.2 Test X-5-o

During the first few interim inspections bundles P and TT appeared to be in good condition except for a small amount of wear which was noted on some sections of

---

+ relative power output is determined from calorimetry of the surrounding lattice sites and varies depending on the number of enriched rods in the vicinity.

wire wrap. On examination in June 1961, an end plate of bundle P was found to be broken. An extra end plate was attached to each end, and one of the spacer rods was replaced. The bundle was re-inserted in the loop during the next reactor cycle. No more interim examinations were held until October 1961, when both bundles were removed from the loop because of high activity in the coolant. Visual inspection did not discover any defect, but a liquid nitrogen immersion followed by a dip in alcohol revealed a split in element TT-4; see Figure 3. (The examination of the failed element TT-4 is described in Section 9 of this report.) The other two elements from bundle TT and the three elements from bundle P were still intact. The extra end plates on bundle P were acting properly, with no sign of excessive corrosion in the crevice between the plates. The failed element from bundle TT was removed and replaced with element TL-2. The irradiation of the repaired bundle was continued, along with bundle P, without any further interim inspections.

Observations made during the final examination were: A grey deposit which covered the surface was easily removable, revealing a shiny black surface on the sheath. Circumferential ridges were visible on the sheaths at positions corresponding to pellet ends. The wire wrap was worn almost half way through in several places. Scratches in the wear areas were transverse, rather than longitudinal. On elements TT-1 and TT-3 the wire wrap was broken at the position of a weld. Other welds on these elements were of poor quality, having many cracks that were observed before irradiation.

6.2 Mensuration

6.2.1 Methods

Tests CR-V-k, CR-V-m, CR-V-n

The diameters of the elements from these tests were measured with normal micrometer calipers, and profiles were taken by passing the element under a dial gauge. Lengths were obtained by supporting each element in a "V" block against a fixed stop, then measuring the length with a depth indicator.

Test X-5-o

Pre-irradiation diameter measurements were made using micrometer calipers across three diameters at 120° to one another at the upper end, midplane and lower end of each element. During the irradiation period interim diameter measurements on the assembled bundles could be made only in one plane (designated 90° in Figure 4). The measurements were made using micrometer calipers at $\frac{1}{4}$ in. intervals along the length of each element. At the final examination after disassembly of

the bundles the elements were held between centers on a converted lathe while diameter measurements were made with a linear displacement transducer as it moved along the elements, producing a continuous diameter trace on a recorder chart (2). Traces were obtained by this method in the same plane as the interim measurements and in another at right angles.

For length measurements the elements were supported in "V" blocks with one end in contact with a fixed end stop and the other with the stylus of a dial indicator. Measurements were made by adding or subtracting the indicator reading from that obtained when the element was replaced with a standard 19 in. length. Measurements represent a mean value of two readings, one measured over the surfaces that were external and the other over surfaces that were internal in the bundle. No interim length measurements could be made on the assembled bundle during the irradiation period. Lengths were corrected for thermal expansion of the sheath by stacking the elements and inserting a thermocouple in the inter-element spacing to obtain an approximate surface temperature. Although the method gave only approximate readings of the sheath temperature, the errors involved would result in less than ±0.002 in. error on the length of an element.

The pre-and the early post-irradiation profiles were obtained by measuring with a dial indicator the perpendicular displacement of the element from a straight rod. Bowing away from the center of the bundle was designated positive. During the later examinations the profiles were obtained by linear displacement transducers, with the output displayed as a continuous profile trace on a recorder chart. Until the bundles were disassembled during the final examination it was possible to measure element profiles only along the surface which faced outward in the bundle. This plane has been designated 0°; after disassembly profiles at 90° to this orientation were also obtained.

6.2.2 Results

The pre-and post-irradiation measurements of the bundles and each element are compared in Table 10. A summary of the results is given below:

CR-V-k Bundles D and E

The four elements containing dished pellets had a mean decrease in length of 0.013 in. The element from each bundle that contained flat-ended pellets had lengthened by 0.078 in. at the low flux and 0.085 in. at the high flux position. No significant diameter changes were noted in bundle D, but bundle E from the high flux position had an

increase in element diameter of 0.003 in. Some circumferential ridging was evident, ranging in height from 0.001 to 0.002 in. on bundle D, and 0.001 to 0.004 in. on bundle E.

CR-V-m Bundles G and H

Bundle G, which had 0.048 in. thick sheaths and was irradiated in the low flux position, had no significant dimensional changes. All the elements from bundle H had increased in length. The element containing flat-ended pellets had lengthened by 0.055 in. while those containing dished pellets had less than one-third of this increase. Bundle H elements had a mean diameter increase of 0.001 in. with ridging ranging in height from 0.001 to 0.003 in.

CR-V-n Bundle K-J

Element K-2, with dished pellets, had a decrease in length of 0.003 in. while element J-1 with flat-ended pellets had lengthened by 0.022 in. There was no significant changes in element diameters and the profiles in the assembled bundle were essentially unchanged. The height of the ridges ranged from 0.001 to 0.002 in.

X-5-o Bundles P and TT

i) Diameters

Bundle P - During interim examinations measurements made in one plane indicated that expansion had occurred at the ends of the elements, particularly the lower end, but that at the middle there had been a decrease in diameter. A sharply localized bulge was evident in the lower quarter of element P-3.

Post-irradiation diameter traces (Figures 4 and 5) demonstrated that the elements of bundle P had become elliptical in cross section at many positions. Generally, on any element the greater increase in diameter was recorded opposite the position of wire wrap in the diameter trace taken at 90° rotation. At the middles and upper ends (U end in Figures) there was a mean diameter increase of 0.002 in. and at the lower ends a mean increase of 0.002 in. in P-1 and 0.006 in. in P-3. There were bulges in elements P-2 and P-3 where localized regions of increased diameter were noted. In element P-2 these were evident only in the 90° plane (Figure 4) at about 4 in. from each end; the maximum increase was 0.014 in. Two bulges were noted on element P-3, one at 2 in. and the other at 6.5 in. from the lower end. Diameter measurements made at these two points have been plotted along polar co-ordinates in Figure 6. Expansion had occurred in all directions and a maximum diameter increase of 0.023 in. was measured.

Ridging at the pellet interfaces, which ranged in height from 0.001 to 0.003 in., was fairly uniform in element P-1 but was less uniform in elements P-2 and P-3.

Bundle TT

No significant diameter changes were noted in the original two elements. The diameter of the replacement element TL-2, which had a thicker sheath, appeared to have decreased by 0.002 in.

At pellet interfaces all elements had circumferential ridges ranging in height from 0.001 to 0.003 in., except element TL-2 which had no ridging at the lower end.

ii) Lengths

The mean increase in bundle P elements was 0.055 in., ranging from 0.050 in. in element P-1 to 0.060 in. in element P-3.

The two elements, TT-1 and TT-3, which remained in bundle TT throughout the experiment had length increases of 0.090 in.. The failed element TT-4 had lengthened by 0.050 in. The thicker sheathed element TL-2, which replaced the latter, had increased by only 0.002 in.

iii) Profiles

After the first irradiation a pronounced bow was observed in element P-1, and a depression recorded at the lower end of P-3, but thereafter the contour of the elements did not alter, as shown in Figures 7 and 8. In the other elements any changes were small. An exception was element TT-1, where positive bowing was observed at the first post-irradiation examination but all subsequent examinations revealed profiles similar to that obtained at the final examination.

After disassembly of the bundles any relaxation which was observed resulted in outward movement at the midplane to give increased outward or decreased inward bowing.

6.3 Fission Gas Release

Each element was punctured under vacuum and the released gases collected on liquid nitrogen cooled charcoal traps. The xenon was separated from the krypton plus argon and the gases analysed by mass spectrometer by Lounsbury and Crocker. The amounts of gases collected are listed in Table 11. The xenon formed during irradiation was taken as 27 ml/MWd (3). Based on this figure the percentage xenon released from each element was calculated and is included in Table 11.

6.4 Disposition of Uranium Oxide

Each element was sectioned at various locations along its length and the UO_2 examined under a stereomicroscope. Observations are listed in Table 12. Representative sections are shown in Figures 9 to 17. The areas of discernible grain growth were measured and on Figure 2 the disposition of the UO_2 is illustrated.

6.5 Condition of Zircaloy Sheathing

Samples of the sheathing from bundle K from CR-V-n, plus P and TT of X-5-o were analyzed for hydrogen content by Ashley. The locations of the samples and the hydrogen contents are given on Figures 18, 19 and 20. Shielded metallographic facilities were not available for examination of components from the CR-V-k and CR-V-m tests. An examination of the hydrogen distribution of sheathing from element K-2 of CR-V-n was reported earlier (4), and is summarized in Table 13, along with results of the metallographic examination of bundles P and TT. Typical observations are illustrated in Figures 21 to 25. Observations on the failed element TT-4 are given in section 7 of this report.

Rings of sheathing were cut from each element of bundle P and TT. Room temperature transverse tensile tests (5) showed that the ultimate strength had increased, but the ductility had decreased substantially compared to unirradiated tubing, as illustrated in Figure 26. Tests carried out at 280°C showed a decreased U.T.S. but also had very low ductility. Detailed results, taken from reference 5 are given in Table 14.

7. EXAMINATION OF FAILED ELEMENT TT-4

7.1 Visual

The surface was a mottled dark grey, and had a rough texture. Rubbing with a cloth dipped in alcohol removed some loosely adhering crud but did not significantly alter the appearance. Decrudding of a short section by a 15 minute dip in a 2:5:93 solution of oxalic acid:nitric acid:water at 75°C did not change the appearance.

The element had a 0.75 in. long crack in the sheath at a point approximately five inches from the lower end. The crack was longitudinal and appeared to pass through a wire wrap weld (but see below). The sheath showed no ductility, and the crack had opened only 0.001 in., as shown in Figure 3. Diameter measurements at the failure were within 0.001 in. of the pre-irradiation dimensions.

7.2 Wire Wrap

During destructive examination of more recent fuel elements wire wrap can be removed in long lengths because fracture occurs preferentially at the weld. On TT-4, however, a large bonded area at the weld, combined with deep fissures in the wire, caused the wire to break between welds leaving small lengths still attached to the sheath. Removal of the wire near the defect revealed that the main crack did not pass through the weld but passed around the fusion zone, and a smaller crack went around the other side of the weld area.

7.3 Leak Testing

The section containing the split was removed from element TT-4. The cut face of each element end was sealed with a greased rubber stopper; the ends were dipped in liquid nitrogen, then immersed in alcohol. No leaks were detected; in particular the end caps and circumferential closure welds had maintained their integrity.

7.4 Metallographic Examination

For comparison with the post-irradiation results pertinent data of the sheathing before irradiation are given in Appendix 1 of this report.

All irradiated sections exhibited hydriding. Near the defect the highest concentrations were observed in the inside surfaces, with areas of almost pure ZrH_2 being observed, as shown in Figure 27. The defect went through one of the areas of highest concentration illustrated in Figure 28, and was not related in any way to the heat affected zone of the weld; see Figure 29. Smaller cracks which did not penetrate the sheath were observed in the ZrH_2 rich areas.

In regions where localized hydriding had not occurred on the inside surface, the hydrogen distribution was similar to that observed in the intact elements from the same bundle, as shown in Figure 30.

All wire wrap welds examined appeared to be sound, with no observable segregation of ZrH_2.

A longitudinal section through the center of the upper end cap revealed only a few hydride platelets, but a section through the lower end cap showed appreciable hydriding; see Figure 31a. No defects were observed. The longitudinal directionality of the hydride precipitation resulted from the original bar reduction. The white band

at the fuel/end-plug interface is essentially free of hydride. The marked area in Figure 31a exhibiting extensive reaction at the UO_2/Zircaloy interface is shown at higher magnification in Figure 31b.

The UO_2 fuel exhibited the same extent of grain growth as observed in the intact element TT-1 and TT-3. Examination of the fuel in the outer annulus revealed that intergranular cracking had occurred.

8. DISCUSSION

8.1 Sheath Deformation

Elements from bundles P and E had larger diametral expansions than the other trefoil elements, but when the expansion plus the original diametral clearance for each element is considered the sums are constant except for bundle P, which are noticeably larger. Justification for the use of the sum of clearance plus expansion was given by Hydraulic Rabbit tests, which showed that when the diameters of elements increased the sum of the expansion plus clearance was nearly constant for a given power output. The effect is further illustrated within bundle D, where the two elements with 0.0075 in. clearance had reduced in diameter, whereas the element with 0.0055 in. clearance had expanded.

The reason for the larger expansions of P-1, P-2 and P-3 has not been established. The Hydraulic Rabbit tests showed that increased power ratings resulted in larger expansions. However the peak ratings of bundle P was lower than that of bundles E and TT, and only marginally higher than that of the other bundles. The interim measurements of bundle P elements suggested a progressive diametral increase. Perhaps the final diameters are larger than normal because of relocation of the fuel during the interim examination, thereby removing or diminishing the diametral clearance. The possibility was considered that swelling of the fuel by accumulation of fission product gases caused the increased expansion, but micro-examination at 1000 magnifications showed no gas bubbles.

The length changes of the CR-V-k elements were the first results to show the effectiveness of pellet-end dishing in controlling the axial expansion of fuel elements, by providing dispersed voidage to accommodate thermal expansion of the UO_2. The effect was further explored in the later trefoil tests and in concurrent irradiations in other loops (7). A plot of the measured extension for a specified depth of dishing is given on Figure 32. The

extension decreases with increased depth of dishing, but is not appreciably affected by heat rating. The length increases of elements with 0.1 in. shoulder width on the pellet end dishing are higher than those of bundles D and E which had the same depth of dishing but had no shoulders.

The influence of diametral clearance on axial extension was not studied in the trefoil irradiations. Other tests, by Notley (8), have shown that when there is good diametral contact, then there is very little relative longitudinal movement between the UO_2 pellets and a thin Zircaloy-2 sheath irradiated in pressurized water. The present results are compatible with this, but the expansion of element H-1 compared to D-29 and E-34 suggests that an axial clearance can have some effect in reducing the length increase. These early results, combined with later irradiations, have led to the development of a model for sheath deformation where the diametral and axial changes are related. The UO_2 pellets are considered to have a plastic core, surrounded by a cracked, but non-plastic annulus. Diametral expansion varies directly with increased heat rating and inversely with fuel to sheath gap. Axial expansions of dished pellets are governed by the temperature of the shoulder of the pellet dishing, or in flat pellets by the thermal expansion of the innermost non-plastic ring of UO_2, taken to be approximately 1000°C. When there is firm contact between the fuel and sheath, and a temperature of 1000°C has been attained, increased heat ratings have negligible effect on the length extension. If the diametral clearance is sufficiently large that there is not firm contact between the fuel and sheath the element can elongate much more, setting up multiaxial forces which can reduce the diameter of the sheath.

The circumferential ridges varied in height from zero to 0.004 in., with the higher readings being recorded on elements with the highest heat ratings. This is in agreement with other tests (9), where the ridge height was found to vary almost linearly with heat rating, and was little influenced by sheath thickness and diametral clearance. The ridge heights of bundle P elements did not increase with prolonged exposure. It has been surmised that the ridges form early in an irradiation and remain unchanged throughout the test. The integrity of the bundle P elements gives credence to this, since it is unlikely that the relatively brittle sheathing would have survived reforming of the ridges at each of the 391 thermal cycles.

8.2 Disposition of Uranium Oxide

The uranium oxide pellets were cracked, some faintly and some with prominent radial and circumferential

cracks. The grain structures which were observed during the post-irradiation examinations ranged between no apparent change from the unirradiated material (bundle D), to extensive columnar growth at the lower end of bundle P. From measurements of discernible grain growth+ and the heat ratings of the individual elements, values of K (400°C, T_g) were calculated by a method given by MacEwan (10). This method, based on an activation energy of grain growth in UO_2 of 110 k cal/mole, takes into account the relative time at different power levels and the rate of grain growth at the temperatures associated with each power output. The resulting values of time- and temperature-weighted average integrated thermal conductivity to the position of grain growth are given in Table 9. More recent tests of approximately two months irradiation of 95% theoretical density UO_2 have resulted in values of K (400°C, T_g) = 33 ± 3 W/cm (11). Variations of the present data from this average can be explained by variations in the grain growth characteristics of the different batches of uranium oxide; the short duration of the CR-V-k irradiation; the low density of the UO_2 in bundles G and H, and element J-1; and the very long duration of the bundle P and TT irradiations.

MacEwan has shown a standard deveation of 150°C, on a mean of 1550°C, for the temperature required to produce 25 μm grain size in a specified time (11). This would be equivalent to 5 W/cm on K (T_s,T_g), and could account for all the differences. Other sources of error could be in the estimated level of, and time at, the peak heat ratings, and the constant associated with the equation used in calculating the effect of such long duration irradiation on the grain growth of UO_2. Corrections for density were made with the empirical relationship developed by Loeb and discussed by Ross (11); $k_m = (1-nP)\ k_t$ where k_m is the measured thermal conductivity, k_t the conductivity of theoretically dense UO_2 and P the percentage porosity. "n" can vary from 0 to 3 depending upon the shape of the porosity and the temperature. For the corrections listed on Table 9, n was taken as 2, but other values might have been more appropriate. Another discrepancy could be variation in the heat transfer

---

+ Taken to be 25 μm diameter grains in the 4X magnification photographs obtained from the stereo-camera.

coefficient between the fuel and sheath in different elements due to changes in surface roughness and contact pressure.

As shown in the final column of Table 9, when the corrections are considered, the values of K (400°C, T_g) are in much better agreement with the more recent results. They also agree well with normalized values from the X-2-t tests (12) which ranged from 28 to 33 W/cm after an irradiation of 12800 hours, and the X-2-s test (13) which had an exposure of 2800 hours and had values of K (400°C, T_g) of 26 to 31 W/cm.

8.3 Fission Gas Release

The most significant result arising from the puncture tests was that element P-2 released about 135 ml of fission product gases (123.6 ml of xenon), yet the element did not fail. Tensile tests of rings of the 0.023 in. thick by 0.95 in. inner diameter tubing showed that at close to operating temperature (280°C) the irradiated Zircaloy had an ultimate tensile strength of 48000 lb/in^2. This would result in a maximum restraint on the gas of 240 atmospheres, including the loop coolant pressure. Since there was no failure in element P-2 during operation, the 135 ml of gas, measured at room temperature, must have been confined to a volume greater than 1.8 cm^3, assuming a mean gas temperature of 700°C. This is compatible with the estimate of Morison (14) that a fuel element with 10.3 g/cm^3 UO_2 operating at K (T_s,T_o) = 40 W/cm, would have an open void space of 2% of the fuel volume, which for element P-2 would be 4 cm^3. Of this, 1 cm^3 would be associated with the radial cracking of the outer annulus of UO_2, another 1 cm^3 with the open porosity of the fuel as fabricated, and the remainder with the voids produced by the columnar grain growth in the centre of the UO_2. If we assume that Morison's estimate is correct and allow for the coolant pressure the tensile stress in the sheath would have been about 8500 lb/in^2. Experiments by Reynolds at San Jose (15) and Harvey and Notley at Chalk River (16) (17) are to measure the pressure inside an operating fuel element.

8.4 Zircaloy Sheathing

The metallographic examination of element K-2 from test CR-V-n was described by Evans and Krenz (3). They concluded from the metallographic evidence and from the reported autoclave treatment that the elements went into the loop with the fuel sheaths containing as much as 120 ppm of hydrogen. Since this amount is

above the solid solubility of hydrogen in Zircaloy at 285°C, the maximum sheath surface temperature, the Zircaloy must have operated for the entire irradiation with a precipitated hydride phase near the outer layer.

The bundle P elements received the same autoclave treatment as those of bundle K, and it was expected that they too would have had a high initial hydrogen content. However, analysis of archive tubing which supposedly received the same treatment, showed only 40 ppm. Therefore there is some ambiguity concerning the level of the starting hydrogen in the bundle P sheathing. Post-irradiation analyses, and the metallographic evidence showed that there was a large difference in hydrogen content in different sections of the sheath, with the lowest analysis being 35.6 ppm and the highest, 182 ppm. As shown on Figure 19, there was no pattern to the extent of hydrogen pickup with high concentrations being observed at either end, and at the midpoint of the different elements. According to laboratory tests by Dalgaard (18) a standard Zircaloy-2 corrosion specimen of 0.015 in. thick tubing, exposed on one side only for the duration of the bundle P test, should pick up 32 ppm. This would be equivalent to a pick-up of 21 ppm in the 0.023 in. thick sheathing of bundle P. Thus the final hydrogen content, based on the archive analyses would have been expected to be approximately 60 ppm. Several analyses did give about 60 ppm, suggesting that these areas represent a normal corrosion rate. The higher hydrogen content in other areas may be due to poor surface preparation prior to autoclaving or to impurities known to be present during the first autoclave test. Recent work at Chalk River (19) has shown that traces of pickle stain or other sources of contamination, can have a profound effect on the oxidation rate and hence the hydrogen content. The oxide film thicknesses ranged from 1.5 to 5 μm. From autoclave tests on well prepared specimens, a film thickness of 1 to 2 μm would be expected on the bundle P sheathing. A film thickness of 5 μm would be associated with a hydrogen pick-up of about 175 ppm, in reasonable agreement with the higher values recorded for bundle P. These figures tend to confirm the hypothesis of poor surface preparation leading to the high hydrogen contents. However, in metallography it was not possible to obtain consistent correlation between areas of high ZrH_2 concentration and thick oxide films, possibly because some of the ZrO_2 may have been knocked off when the elements were cut with tubing cutters. No satisfactory explanation can be given for the analysis of 35.6 ppm of hydrogen, particularly since the opposite side of the same specimen had 160 ppm.

Marshall and Louthan (20) have studied the tensile properties of Zircaloy-4 with oriented hydrides.

They have defined a parameter H-effective which is the product of the fraction of hydride platelets that are normal (i.e. 50 to 90°) to the applied stress, and the total hydride content. As the total hydrogen increased above 50 ppm the strength began to decrease, but the amount of decrease varied with hydride orientation. The ductility of the material decreased with increasing hydrogen, and all specimens containing more than 50 ppm H-effective exhibited no macroscopic ductility. Room temperature ring tensile tests of bundle P sheathing generally showed increased strength and a marked decrease in ductility. A few specimens failed in a completely brittle manner, some with increased and some with decreased strengths compared with the unirradiated material. The total hydride content varied from 60 to 160 ppm and was oriented in a Widmanstätten-like structure with the principal direction about 45° to the surface. The increased tensile strength can be attributed to radiation damage (21), with perhaps a small contribution from the hydrogen content (22). The completely brittle failures and the lower tensile strengths are considered to be due to higher concentrations of hydride platelets precipitated normal to the surface, i.e. H-effective > 50 ppm.

All tests on elements TT-1 and TT-3 showed increased strength. However, the ductility was lower than in tensile specimens irradiated to the same fast neutron exposure in a fast neutron convertor rod (21). The differences could be due to the method of testing, although unirradiated rings of sheathing showed normal strength and ductility. Similarly, sheathing from TL-2, which had much less irradiation than TT-1 and TT-3, had only a slight increase in strength and there was still good ductility. The hydride platelets of TT-1 and TT-3 were parallel to the sheath surface and should not have appreciably affected the tensile properties. Other differences between the test specimens and the fuel sheathing could be the effect of bi-axial stressing on the strength of the Zircaloy-2, the presence of minor cracks in the interior surface of the tubing, and perhaps the close contact of the fuel and sheathing resulting in significant bombardment of a thin surface layer by fission fragments, which might also reduce the ductility.

Rings containing the wire wrap welds had no difference in strength compared to those taken between welds, showing that the weld was not lowering the integrity of the material.

The hydride distribution in the end cap and end plate, illustrated in Figure 25, can be explained from the geometry and known temperature profiles in the end cap; i.e. the larger surface to volume ratio of the sheaths relative to the end cap would result in a faster increase of hydrogen concentration in the sheath. This

would establish a concentration gradient which would drive hydrogen into the end cap. In the end cap the hydrogen would diffuse to the cooler regions at the shoulders. The temperature gradient between the shoulders and the spigot is not known. Hydrogen picked up at the spigot might diffuse towards the shoulders, as suggested for elements of smaller diameter (23). However the size and geometry of the spigot should result in sufficiently rapid pickup that considerable hydride precipitation is apparent; see Figure 25. The orientation of the hydride platelets in the spigot and end plate is due to the fabrication procedures. If the precipitation were normal instead of parallel to the plate surfaces the material would be much more brittle; hence, fabrication processes for end plates, such as casting, should be scrutinized for possible adverse hydride precipitation.

The brittle nature of the failure of the lower end plate of bundle P is considered to be due to excessive hydride content. Two analyses of the irradiated material gave results of about 400 ppm. The majority of this pickup is thought to have occurred during the first autoclaving, when this end plate was close to the contamination in the bottom of the autoclave. The exact time of the failure can not be fixed, but because of the shiny white surfaces of the fracture faces it is known that the break occurred after the element was removed from the high temperature coolant, when all the hydrogen present would be precipitated as ZrH_2 platelets.

9. FAILURE OF ELEMENT TT-4

Element TT-4 failed after 10860 hours of loop operation, and a burn-up of approximately 4500 MWd/te of U. The observations from the examination and other pertinent data are summarized below:

A. Pre-Irradiation

1. Element TT-4 had 0.001 in. thinner sheath than elements TT-1 and TT-3.

2. The pellets were sintered at 1650°C and the moisture content was very low.

3. The unirradiated Zircaloy-2 had good ductility and a U.T.S. of 66000 lb/in^2. The material was α-annealed by the manufacturer.

4. The sheaths of all elements received the same autoclave treatment, and entered the reactor with about 40 ppm of H_2.

5. The wire wrap welds had many deep fissures caused by blow-out of molten material.

B. Operation

The power output of bundle TT had increased from 54 kW to 83 kW when it was moved into the higher flux position, i.e. an increase of 52%. During the cycle when the element failed the loop temperature had been reduced to 190°C from the normal 260°C. At this temperature the terminal solid solubility of hydrogen in Zircaloy-2 is about 30 ppm (24). After the failure was noted the loop temperature was raised to 215°C, and operation continued for four days.

C. Dimensions

1. There was no significant diametral expansion in the intact elements. At the position of the split in TT-4 the diameter was within 0.001 in. of the pre-irradiation data. The length change of 0.050 in. for TT-4 was slightly less than the changes of TT-1 and TT-3 but almost identical to those from P-1, P-2 and P-3.

2. Bundle P elements, with similar diametral clearances, and irradiated continuously at similar power ratings as the maximum rating of bundle TT, had expanded 0.002 to 0.005 in.

D. Condition of TT-4

1. The Zircaloy was a mottled grey with no large area of accelerated corrosion.

2. A 0.75 in. long longitudinal split occurred five inches from the lower end.

3. The split was of a brittle nature, and passed around a wire wrap weld.

4. The end caps and end closure welds were intact.

E. Metallography

1. Metallographic examination of the intact elements showed no signs of a defect.

2. In TT-1 and TT-3 the hydride platelets were oriented parallel to the sheath surface. Chemical analyses gave hydrogen contents between 70 and 90 ppm.

3. Element TT-4 had very high concentrations of hydride near the defect, i.e.: up to 1435 ppm. The remainder of the sheath, particularly near the ends, had higher concentrations than observed in elements TT-1 and TT-3. At the defect the hydride platelets were normal to the sheath, but away from the defect they were predominantly parallel to the sheath.

4. The extent of grain growth in the UO_2 was the same as that observed in the other elements. Fuel in the outer annulus had extensive intergranular cracking.

F. Tensile Tests

1. Ring tensile tests on irradiated sheathing from bundle TT showed it to have increased strength and very little ductility.

2. The presence of a wire wrap weld had no effect on the tensile strength or ductility of a ring section of sheath.

From the above information a tentative mechanism for the failure of element TT-4 can be proposed; viz: When the power output was raised by 50%, additional stress was imposed on the sheath by the thermal expansion of the UO_2. Because of the lower coolant temperature there would have been some hydride precipitated. For seven days prior to the failure the sheath was under increased tangential stress because of the higher heat ratings, which might have caused some of the precipitation to be normal to the surface; and combined with the reduction in ductility of the Zircaloy resulting from radiation damage, the sheath could not yield and split in a brittle manner.

The large amount of hydrogen in the sheath was not reflected in the thickness of the ZrO_2 films. Similarly large amounts of hydrogen have been observed in other tests without the corresponding amounts of ZrO_2 e.g. test X-507 element ENW (25), and several BAPL elements reported by Markowitz (26), who states that only radiolysis can produce hydrogen at a rate sufficient to produce the hydrogen contents observed. He considered, but rejected water corrosion, steam oxidation of the fuel, and stripping of dissolved hydrogen from the coolant as possible methods.

10. CONCLUSIONS

1. The irradiation testing of prototype NPD fuel has demonstrated that 1 in. outer diameter, 19 in. long UO_2 elements, sheathed in Zircaloy-2 with a thickness to diameter ratio of 0.02, may be irradiated at $\int k d\theta$ = 40 W/cm for 18000 hours to an exposure of ~ 9000 MWd/tonne U without adverse effect.

2. The early irradiations established that dishing pellet ends was an effective method of controlling length expansion. The later tests at higher ratings and longer exposure confirmed the earlier results, and showed that coalescence of the pellets did not result in unusual dimensional changes.

3. Wire wrapping elements proved to be an effective method of maintaining bundle spacing. No deterioration of the sheath was noted at any wire wrap spot weld, and there was no evidence of fretting corrosion under the wires which were secured at the ends only.

4. Up to 135 cm^3 of fission product gases were contained within an element with an estimated free volume of 2 to 4 cm^3 without failure of the cladding. In this element, irradiated to 9100 MWd/tonne at $\int kd\theta$ = 40 W/cm, 27% of the fission product xenon was released in a vacuum puncture test.

5. The grain growth behaviour of the UO_2 was in reasonable agreement with out-of pile data when corrections for density and duration of irradiation were considered. Discrepancies which did occur could be explained by differences in the growth characteristics of the batches of UO_2, heat transfer between the fuel and sheath, and incorrect estimations of the time at, and the level of the peak heat ratings.

6. Some sections of the sheathing had hydrogen in the amount predicted from published out-of-pile corrosion rates of Zircaloy-2; other sections contained much more hydrogen. The excessive hydrogen may be attributable to the pre-irradiation autoclave treatment, and to the lack of a good pre-transition ZrO_2 film on the surface of the elements.

7. The fracture of an end plate during handling of bundle P was due to very high hydrogen content, the most of which was picked up during autoclaving.

8. A failure in element TT-4 was caused by increased stress due to a higher heat rating, combined with low ductility of the Zircaloy-2 due to two reasons: Irradiation damage and precipitation of ZrH_2 because of a lower coolant temperature.

9. The failure of a high burn-up element did not lead to excessive activity release, nor was there a catastrophic disintegration of the components which would have led to jamming in the fuel channel of a power reactor.

11. ACKNOWLEDGEMENT

Acknowledgement is extended to R.F. Fortune, G.R. Fanjoy, and A.G. Cracknell of Canadian General Electric, plus D. Nishimura and A.D. Lane of AECL for their work during the irradiation of the bundles; to R.W. Ashley for

the hydrogen analyses; to R.W. Durham for the burn-up results; to G.W. Parry for the metallography; to D.C. Fleming for the tensile values; and to R.D. MacDonald and J.A.L. Robertson for valuable discussions on the interpretation of the data.

12. REFERENCES

1. Test CR-V-k - reports in series Exp-NRX-900
Test CR-V-m - reports in series Exp-NRX-2600
Test CR-V-n - reports in series Exp-NRX-3100
Test X-5-o - reports in series Exp-NRX-4100

2. Christie, J., and Bain, A.S., "Dimensional Measurements in Irradiated Fuel Bundles Using Differential Transformer Instrumentation" AECL-1603, August 1963.

3. Lewis, W.B. "The Return of Escaped Fission Product Gases to UO_2" AECL-964, January 1960.

4. Evans, W. and Krenz, F.H., "Analysis of H Pick-up in Sheath of Specimen K-2" Exp-NRX-3105. Not for Publication. March 1960.

5. Fleming, D.C., "Transverse Tensile Tests in Zircaloy-2 from Long Term Irradiation Fuel Bundles" AECL-CRGM-1160, Proprietary. July 1963.

6. Bain, A.S., Robertson, J.A.L. and Ridal A., "UO_2 Irradiations of Short Duration - Part II" AECL-1192, February 1961.

7. Robertson, J.A.L., Bain, A.S., Allison, G.M. and Stevens, W.H., "Irradiation Behaviour of UO_2 Fuel Elements" Nuclear Metallurgy VI, 45, November 1959.

8. Notley, M.J.F., "The Relative Axial Expansions Under Irradiation of Stacks of UO_2 Pellets in Zircaloy Sheaths" AECL-1598, August 1962.

9. Bain, A.S., "Cracking and Bulk Movement in UO_2 Fuel Elements" CRFD-1156, September 1963.

10. MacEwan, J.R. "Private Communication to Bain, A.S., March 20, 1963.

11. Robertson, J.A.L., Ross, A.M., Notley, M.J.F., and MacEwan, J.R. "Temperature Distribution in UO_2 Fuel Elements" Journal Nuclear Materials 7 No. 3, 1962.

12. MacDonald, R.D. and Parry, G.W., "Zircaloy-2 Clad UO_2 Fuel Elements Irradiated to a Maximum Burn-up of 10,000 MWd/tonne U." Exp-NRX-2906 to be issued.

13. MacDonald, R.D. and Bain, A.S. "Irradiation of Zircaloy-2 Clad UO_2 to Study Sheath Deformation" AECL-1685, December 1962.

14. Morison, W.G. "Fission Gas Release from UO_2 in CANDU Fuel Elements" TDSI-28, not for publication, November 1960.

15. Reynolds, M.B. "Experimental Measurement of Fission Gas Pressure in Operating Fuel Elements" Trans. Amer. Nuc. Soc. 5, 2, November 1962.

16. Harvey, A. "UO_2 Pellet Rod MK IX" Exp-NRX-7801, Not for Publication.

17. Notley, M.J.F. and Harvey, A. "An Irradiation to Measure the Gas Pressure Inside Operating Fuel Elements" Exp-NRX-51201 - not for publication, June, 1963.

18. Dalgaard, S.B. Private Communication, June 14, 1963.

19. **Dalgaard,** S.B. and McVey, E.G. Chalk River work, to be published.

20. Marshall, R.P. and Louthan, M.R. "Tensile Properties of Zircaloy with Oriented Hydrides" Symposium on Zirconium Alloy Development, Pleasanton, Calf. November, 1962.

21. Howe, L.M. and Thomas, W.R. "The Effect of Neutron Irradiation in the Tensile Properties of Zircaloy-2" J. Nuc. Mat. 2, 248, 1960.

22. Sawatzky, A. "The Mechanical Properties of Hydrided Zr-2.5 wt% Nb and Hydrided Cold-Worked Zircaloy-2" AECL-GMI-15, Not for Publication, September, 1962.

23. Daniel, A.R. and Bain, A.S. "Distribution of Hydrogen in Irradiated Zircaloy-2 Sheaths" Exp-NR**U**-1314, Not for Publication, 1961.

24. Sawatzky, A. "The Diffusion and Solubility of Hydrogen in the Alpha-Phase of Zircaloy-2" J. of Nuc. Mat. 2, No. 1, 62, 1960.

25. Hardy, D.G. Chalk River work to be reported.

26. Markowitz, J.M. "Internal Zirconium Hydride Formation in Zircaloy Fuel Element Cladding Under Irradiation" WAPD-TM-351, May, 1963.

APPENDIX I

PRE-IRRADIATION DATA FOR ELEMENT TT-4

1. Quality of the As-Received Tubing

The lengths of sheathing used for element fabrication were examined at AECL and CGE. The as-received tubing had been pickled inside and out. Fluorescent penetrant testing (Zyglo), boroscope examination and leak testing failed to reveal defects. At this time ultrasonic testing was unreliable and inspection of the tubing by two different methods produced contradictory results. However, any indications that were obtained did not coincide with the failure in element TT-4.

2. Pickling

Four pickles were carried out during processing of element TT-4.

(a) A 0.002 inch removal from the outer surface before welding.
(b) A 0.002 inch removal from the outer surface after welding.
(c)&(d) Two 0.0005 inch removals in an unsuccessful attempt to remove scratches produced during ultrasonic testing.

3. Autoclaving

Steam autoclaving at 400°C and 800 lbs/in^2 for 72 hours was intended but the pressure fell to 550 lbs/in^2 during the test. It was noted on subsequent examination that:

(a) Faint scratches were visible parallel to some of the wires.
(b) Small areas on the end caps were free of oxide.

4. Hydrogen Content

The material was supplied to the then current specification requirement of < 30 ppm H_2. Two chemical analyses of the as-received material yielded 27 ppm H.

Archive samples autoclaved on both sides yielded 48, 48 and 49 ppm H. It may therefore be assumed that the fuel element entered the reactor with approximately 40 ppm H in the sheath.

5. Fabrication and Assembly

Four elements were made. One identified TT-2 was used for shear testing the wire-wrap welds and the other three TT-1, TT-3 and TT-4 were used to make up the irradiation test bundle. The three one-inch diameter fuel elements were attached to the end plates by riveting and three spacers were attached with stainless steel bolts.

Practically all the wire-wrap welds on element TT-4 had deep fissures with the worst being ~ 0.020 inches deep. TT-1 and TT-3 were better although some fissures were still evident. The production of these fissures was due to arcing at the periphery of the electrode followed by indentation and displacement of the liquid metal produced by arcing. The probability of the fissures propagating is much less than for a crack because of the large radii at their extremes.

6. Metallographic Examination of Archive Wire-Wrapped Autoclave Sample

Sections were taken through three representative welds. No defects were found in the sheathing wall. The bonded length was good and the extent of the heat-affected zone was moderate (see Figure 33).

The longitudinal section shown in Figure 34, illustrates the discontinuities that can occur in a weld.

TABLE 1

DESIGNATION OF TESTS

Test	Bundles	Main Objectives	Design Changes	References
CR-V-k	D E	1. Feasibility test of trefoil design 2. Calibration to determine enrichment for heat ratings required 3. Stability of thin sheathing that was not self-supporting 4. Effect of pellet dishing in controlling axial expansion 5. Fission gas release		Exp-NRX- 900
CR-V-m	G H	1. Effect of higher burnup on stability of fuel elements 2. Effect of varying diametral clearance 3. Effect of sheath thickness on axial and diametral expansion 4. Continued study on effect of pellet dishing in controlling axial expansion 5. Release of fission product gas	Sheath thickness increased in bundle G. Pellet dishing removed in thick sheathed elements. Axial clearance increased in both bundles and diametral clearance increased in bundle G.	Exp-NRX-2600
CR-V-n	K-J	1. Behaviour of high density fuel with respect to gas release, thermal conductivity and expansion	Density of UO_2 raised; pellet dishing reduced; diametral clearance returned to original amount. Elements rivetted to end plates	Exp-NRX-3100
X-5-o	P TT	1. Long duration irradiation of prototype fuel irradiated at NPD-2 heat ratings, and higher	Diametral and axial clearance reduced. Wire wrap welded onto sheath of TT. Elements rivetted to end plates in bundle P.	Exp-NRX-4100

TABLE 2

UO_2 FABRICATION CONDITIONS

Test	CR-V-k	CR-V-m Bundle G	CR-V-m Bundle H	CR-V-n Bundle K	CR-V-n & X-5-o Bundle P	X-5-o Bundle TT
UO_2 Powder batch	P95	P88	P102	P88AB	P103A	P112
Grind	-100 mesh	-60 mesh	-100 mesh	-100 mesh	-100 mesh	-100 mesh
Pre-Press (lb/in^2)	10,000	10,000	10,000	20,000	10,000	20,000
Granulate	-20 mesh	-20 mesh	-20 mesh	-20 mesh	-20 mesh	-20 mesh
Final Press (lb/in^2)	20,000	20,000	20,000 with flat or concave die	40,000 with flat or concave die	20,000 with flat or concave die	40,000
Sinter Time (h)	2.5	4	2.5	2.5	2.5	3
Temp (°C)	1650-1675	1650	1650	1650	1650	1650
Atmos.	cracked NH_3	cracked NH_3	cracked NH_3	cracked NH_3	cracked NH_3	cracked NH_3
Centreless grind (in.)	±0.0005	±0.0005	±0.0005	±0.0005	±0.0005	±0.0005
Final finish	grind dishing lap flat ends	lap flat ends	----	----	----	----
ZIRCALOY-2 SPECIFICATIONS						
Cold work (%)	not known	15-20	10-15	15-20	10-15	α-annealed
Autoclave	water at 680°F 2750 (lb/in^2)	steam at 750°F 1200 (lb/in^2)	steam at 750°F 1200 (lb/in^2)	steam at 750°F 800 (lb/in^2)	steam at 750°F 800 (lb/in^2)	steam at 750°F 800 dropping to 500 (lb/in^2)
	7 days	90 hours	90 hours	24 hours(a)	24 hours(a)	72 hours

(a) Autoclave controller failed and autoclave was opened. All elements were extensively covered with white corrosion product which were removed with vapour blasting. Elements were pickled, then re-autoclaved in steam at 750°F, 800 (lb/in^2) for 18 hours. Excessive corrosion in the first test was due to welding slag and a monel shelf inside the autoclave.

TABLE 3

SPECIMENS DETAILS

Test	Specimen Code	Zircaloy-2 Sheath: Length Overall	Average O.D.	Average I.D.	Nominal Thickness	UO_2 Fuel: Batch No.	No. of Pellets	Total Weight UO_2	Enrichment[a]	Density	Pellet[b] Dishing	Stacked Length	Clearances: Axial	Diametral
		(in.)	(in.)	(in.)	(in.)			(g)	(wt% U-235 in total U)	(g/cm^3)	(in./in.)	(in.)	(in.)	(in.)
CR-V-k	D29	18.954	1.0015	0.9545	0.023	P 95	38	2172	2.278	10.45	flat	18.001	0.006	0.0075
	D32	18.939	1.0018	0.9548	0.023	P 95	38	2083	2.278	10.17	0.030	17.954	0.001	0.0077
	D12	18.951	1.0018	0.9528	0.023	P 95	39	2091	2.278	10.38	0.064	17.996	0.019	0.0058
	E34	18.942	1.0025	0.9540	0.024	P 95	39	2182	2.278	10.44	flat	18.000	0.008	0.004
	E15	18.948	1.0017	0.9533	0.024	P 95	38	2135	2.278	10.36	0.030	17.977	0.008	0.0033
	E25	18.940	1.0030	0.9539	0.024	P 95	38	2104	2.278	10.36	0.064	17.993	0.003	0.004
CR-V-m	G-1	19.235	0.9952	0.8989	0.048	P 88	35	1853	2.27	10.11	flat	17.944	0.098	0.0077
	G-2	19.232	0.9956	0.8988	0.048	P 88	34	1832	2.27	10.07	flat	17.908	0.063	0.0099
	G-3	19.228	0.9957	0.8989	0.048	P 88	35	1787	2.27	9.91	flat	17.950	0.088	0.0121
	H-1	19.228	1.0037	0.9529	0.025	P102	36	2082	1.633	10.11	flat	17.925	0.073	0.0051
	H-2	19.232	1.0037	0.9537	0.025	P102	35	2052	1.633	10.21	0.064	17.972	0.016	0.0058
	H-3	19.229	1.0036	0.9530	0.025	P102	35	2080	1.633	10.18	0.030	17.968	0.013	0.0057
CR-V-n	K-1	18.937	0.9974	0.9288	0.034	P 88 AB	36	2089	2.265	10.70	0.015	17.961	0.018	0.007
	K-2	18.940	0.9967	0.9283	0.034	P 88 AB	36	2090	2.265	10.70	0.015	17.960	0.025	0.0065
	J-1	18.936	0.9934	0.8993	0.047	P 88	35	1856	2.265	10.09	flat	17.950	0.050	0.0068
X-5-o	P-1	18.935	0.9999	0.9534	0.023	P103 A	37	2136	1.646	10.38	0.015	17.953	0.000	0.0056
	P-2	18.940	1.0002	0.9532	0.023	P103 A	37	2120	1.646	10.30	0.015	17.925	0.005	0.0054
	P-3	18.939	0.9996	0.9528	0.023	P103 A	37	2122	1.646	10.27	0.015	17.965	0.006	0.0051
X-5-o	TT-1	19.251	0.9954	0.9497	0.023	P112	21	2231	1.642	10.53	0.019	18.585	0.035	0.0060
	TT-3	19.255	0.9959	0.9497	0.023	P112	21	2231	1.642	10.52	0.019	18.596	0.011	0.0057
	(c) TT-4	19.253	0.9959	0.9501	0.023	P112	21	2229	1.642	10.52	0.019	18.605	0.013	0.0062
	(c) TL-2	18.935	1.0003	0.930	0.035	P103	37	2004	1.65	10.35	0.015	17.976	0.004	0.008

(a) Mass spectrometry results.

(b) Bundles D and E did not have any shoulder on the pellet end dishing; the other dished pellets had shoulders of about 0.1 in.

(c) TL-2 was inserted when element TT-4 became defective.

TABLE 4

IRRADIATION HISTORY

Test	Date In	Date Out	Reactor Power Level (MW)	Integrated Reactor Power (MWd)	Equivalent Full Power Days (d)	Total Time of Loop Operation (h)	Thermal Cycles
CR-V-k	Oct.10/58	Oct.27/58	35	571	(a)	402	16
CR-V-m	Dec.14/58	Feb. 9/59	40 (b)	1,622	41.6	1,049	62
CR-V-n Bundle K-J	Mar. 1/59	Nov.16/59	40	8,106	202.6	4,952	141
X-5-o Bundle P	Mar. 1/59	May 22/62	40 to 42 (b)	30,313	740	18,186	391
X-5-o Bundle TT	Nov.17/59	May 22/62	42	20,103	490.6	12,055	214
X-5-o Bundle TT Element TL-2	Mar.23/62	May 22/62	42	2,005	47.8	1,194	27

(a) Reactor was never at full power during CR-V-k test.

(b) Reactor full power was quoted as 40 MW until Jan.18, 1961. At that time, it was discovered that full power had actually been 41.6 MW and the reactor was then adjusted slightly so that full power was 42 MW.

TABLE 5

REACTOR OPERATION DATA FOR TEST CR-V-k

Date	Reactor Power (a) (MW)	Action Taken	Calculated Max. $\int_{T_s}^{T_o} k d\theta$ in Bundle E (W/cm)
0100 hr October 10/58	20	Heat output checked and found to be satisfactory; therefore, power was raised.	
0300 hr October 10/58	25	As above.	
0315 hr October 10/58	30	Heat output checked and was considered to be the maximum allowable. As the poisons increased, the effective heat rating decreased to a value corresponding to $\int k d\theta$ = 44 W/cm; therefore, the power was raised.	49.5 44
1730 hr October 11/58	35	Reactor operated at this power level for the remainder of the cycle.	46
0200 hr October 27/58	0	Reactor shut down and test removed.	

(a) See footnote to Table 4.

TABLE 6

X-5-o IRRADIATION RECORD

Loading	Bundles Included	Date In	Date Out	Examined	Total Hours	Total Reactor MWd	Equivalent Full Power Days
1	TT, OC	Nov. 17	Dec. 15/59	P	487.2	804.7	20.0
2	TT, OC, P	Dec. 17	Dec. 23/59	P, TT, OC	67.9	107.9	2.7
		Dec. 28	Jan. 2/60		47.3	73.3	1.8
		Jan. 12	Jan. 26/60		261.5	431.7	10.7
		Jan. 27	Mar. 22/60		1072.6	1733.5	43.4
				P			
3	TT, OC, P	Mar. 24	May 30/60		1424.2	2362.1	58.1
				P, TT, OC			
4	TT, OC, P	July 5	Aug. 23/60		959.3	1587.5	39.6
5	TT, P	Aug. 24	Aug. 28/60		7.5	8.5	.2
				P, TT			
6	TT, P	Sept. 20	Sept. 30/60		130.1	165.4	4.1
7	TT, P	Sept. 30	Dec. 19/60		1580.3	2595.0	65.0
				P, TT			
8	TT, P	Jan. 3	Feb. 26/61		1119.9	1911.9	46.7
9	TT, P	Mar. 2	April 3/61		720.4	1250.6	29.8
10	TT, P	April 27	May 28/61		759.4	1323.1	31.5
11	TT, P	May 31	June 27/61		557.9	971.1	23.0
				P, broken end plate replaced.			

TABLE 6 CONT'D

X-5-o IRRADIATION RECORD

Loading	Bundles Included	Date In	Date Out	Examined	Total Hours	Total Reactor MWd	Equivalent Full Power Days
12	TT	June 28	July 7/61		160.8	263.6	6.3
	TT	July 10	July 24/61		235.7	385.6	9.2
13	TT, P	July 25	Sept. 18/61		1044.0	1756.8	42.0
14	TT, P	Sept. 21	Oct. 2/61		225.0	365.0	8.7
				P, TT failure in TT-4			
UIF 1	P	Oct. 27	Dec. 19/61		927.5	1591.8	37.9
UIF 2	P	Dec. 19/61	Feb. 19/62		1135.8	1966.9	46.8
UIF 3*	TT, P	Mar. 23	April24/62		646.3	1095.4	26.1
UIF 4*	TT, P	April27	May 22/62		547.4	910.1	21.7

* Element TT-4 replaced by TL-2.

TABLE 7

RELATIVE NEUTRON FLUX SEEN BY TREFOIL BUNDLES

Test	CR-V-k		CR-V-m		CR-V-n and X-5-o		
Bundle	D	E	G	H	K	P	T-T
Position of mid-point of bundle (cm above bottom of calandria)	216	164	222	167	227	(a) 172 (1) 163 (2) 118 (3) 113	(1) 219 (2) 176 (3) 56
Percentage of neutron flux (nominal)	78	98	72	97.5	69	97 (1) 98.5 (2) 97 (3) 95	(1) 73 (2) 96.5 (3) 63
"f" factor of loop	0.0090		0.0094		(b) varied from 0.0085 to 0.0094, average 0.0090 (c) varied from 0.0077 to 0.0095, average 0.0090		
Moderator height (average) (cm)	292		288		289		285 ± 5

(a) Numbered values are for the three different positions in test X-5-o.

(b) "f" factors for test CR-V-n.

(c) "f" factors for test X-5-o.

TABLE 8

POWER OUTPUT OF BUNDLES AND ELEMENTS

Burn-Up Average For Bundle [a]		Bundle Power Time-Average [b]		Bundle Power Peak-Instantaneous	Element Power Per Unit Length At Mid-Point Time-Average		Peak Instantaneous
		Burn-Up	Calorimetry	Calorimetry	Burn-Up	Calorimetry	Calorimetry
(MWd/T U)		(kW)	(kW)	(kW)	(W/cm)	(W/cm)	(W/cm)
D	222 (c)		69.5	73.5		512	541
E	282 (c)		87.5	92.5		645	681
G	510	55	56	65	405	413	479
H	560	67	65	80	494	479	590
K	2430	59	57	65	K1, K2 446	431	491
J	2520				J 406	392	447
P	9120	64.2	63.5	81	473	468	596
TT	4955	54.5	---	83	402		611

(a) Based on 199 MeV/fission.

(b) Based on 182 MeV/fission.

(c) Burn-up of D and E calculated from calorimetric data; the remainder were derived from chemical analyses.

TABLE 9

HEAT RATINGS AT MID-POINT

Bundle	Average from Burn-Up $\int_{T_s}^{T_o} k d\theta$	Peak from Calorimetry	Based on Average Burnup $\int_{T_s}^{T_g} k d\theta$	Estimated T_s[a]	$\int_{400°C}^{T_g} k d\theta$	Correction[b] for Duration	Correction[b] for density	$\int_{400°C}^{T_g} k d\theta$ Normalized[c]
	(W/cm)	(W/cm)	(W/cm)	(°C)	(W/cm)	(W/cm)	(W/cm)	(W/cm)
D	37.2	39.4		no grain growth at mid-point				
E	46.8	49.5	41	390	41	- 3	0	38
G	29.4	34.7	25.5	360	25.0	0	G-1,G-2 +1.5	26.5
							G-3 +3	28.0
H	36.1	43.9	27.8	380	29.0	0	+1.5	30.5
K-1,K-2	32.4	35.6	29.6	360	28.5	+ 2.5	-1.0	30
J	29.4	32.4	25.2	360	24.0	+ 2.5	+1.5	28
P	35.2	44.4	23.0	360	23.5	+ 6	0	29.5
TT	30	45.5	25.7	360	30.0	+ 4	-0.5	33.5

(a) Film drop of 20°C; thermal conductivity of Zircaloy-2 taken as 0.155 W/cm°C; heat transfer coefficient between fuel and sheath taken as 1 $W/cm^2°C$.

(b) See text.

(c) Normalized to 60 day irradiation of 10.5 g/cm^3 UO_2 for comparison with other tests.

TABLE 10

DIMENSIONAL CHANGES IN INCHES[a]

Experiment and Element	Mean O.D. (excluding ridges) Before Irradiation	Mean O.D. (excluding ridges) After Irradiation	Mean O.D. (excluding ridges) Change	Maximum O.D. (excluding ridges)	Mean Length Before Irradiation	Mean Length After Irradiation	Mean Length Change	Height of Circumferential Ridges	Maximum 0° Bow Before Irradiation	Maximum 0° Bow After Irradiation	Maximum 0° Bow After Bundle Disassembly
CR-V-k											
D-29	1.0015	0.9995	- 0.002		18.954	19.032	+ 0.078	0.001			
D-32	1.0018	1.0007	- 0.001		18.939	18.933	- 0.006	0.001 - 0.002			
D-12	1.0018	1.0027	+ 0.001		18.951	18.930	- 0.021	0.001			
E-34	1.0025	1.0065	+ 0.004		18.942	19.027	+ 0.085	0.001 - 0.004			
E-15	1.0017	1.0047	+ 0.003		18.948	18.938	- 0.010	0.001 - 0.003			
E-25	1.0031	1.0065	+ 0.003		18.940	18.926	- 0.014	0.002 - 0.003			
CR-V-m											
G- 1	0.9952	0.9953	nil		18.937	18.940	+ 0.003	Ridges were visible but not measurable i.e. < 0.001			
G- 2	0.9956	0.9957	nil		18.931	18.935	+ 0.004				
G- 3	0.9957	0.9953	nil		18.932	18.936	+ 0.004				
H- 1	1.0037	1.006	+ 0.002		18.940	18.995	+ 0.055	0.001 - 0.003			
H- 2	1.0037	1.005	+ 0.001		18.944	18.958	+ 0.014	0.001 - 0.003			
H- 3	1.0036	1.004	nil		18.939	18.957	+ 0.018	0.001 - 0.002			
CR-V-n											
K- 1	0.9974	0.997	nil		18.937	Not measured		0.001 - 0.002	nil	+ 0.020	+ 0.011
K- 2	0.9967	0.998	+ 0.001		18.940	18.937	- 0.003	0.001 - 0.0015	- 0.015	- 0.019	- 0.012
J- 1	0.9934	0.9925	- 0.001		18.936	18.958	+ 0.022	0.001 - 0.0015	nil	+ 0.008[c] - 0.014[c]	+ 0.008[c] - 0.005[c]
X-5-o											
P- 1	0.9999	1.001	+ 0.001[b]	1.007[b]		Not measured		0.001 - 0.003	+ 0.069	+ 0.060	
		1.003	+ 0.003[b]	1.007[b]		" "		0.001 - 0.003		+ 0.055	
		1.005	+ 0.005[b]	1.009[b]		" "		0.001 - 0.003		+ 0.062	
		1.004	+ 0.004[b]	1.009[b]		" "		0.001 - 0.003		+ 0.062	
		Not measured				" "		0.001 - 0.003		+ 0.055	
		" "				" "		0.001 - 0.003		+ 0.053	
		1.002	+ 0.002	1.005	18.935	18.985	+ 0.050	0.001 - 0.003		+ 0.052	+ 0.051

TABLE 10 CONT'D

DIMENSIONAL CHANGES IN INCHES[a]

Experiment and Element	Mean O.D. (excluding ridges) Before Irradiation	After Irradiation	Change	Maximum O.D. (excluding ridges)	Mean Length Before Irradiation	After Irradiation	Change	Height of Circumferential Ridges	Maximum 0° Bow Before Irradiation	After Irradiation	After Bundle Disassembly
Cont'd.											
X-5-o											
P- 2	1.0002	1.001	+ 0.001[b]	1.006[b]		Not measured		0.001 - 0.002	- 0.015	- 0.026	
		1.003	+ 0.003[b]	1.009[b]		" "		0.001 - 0.002		- 0.023	
		1.004	+ 0.004[b]	1.008[b]		" "		0.001 - 0.002		- 0.016	
		1.006	+ 0.006[b]	1.013[b]		" "		0.001 - 0.002		+ 0.002 / - 0.018[c]	
		Not measured				" "		0.001 - 0.003		+ 0.002 / - 0.021[c]	
		" "				" "		0.001 - 0.003		+ 0.004 / - 0.019[c]	
		1.004	+ 0.004	1.011	18.940	18.995	+ 0.055	0.001 - 0.003		+ 0.005 / - 0.020[c]	+ 0.007 / - 0.013[c]
P- 3	0.9996	1.002	+ 0.002[b]	1.011[b]		Not measured		0.001 - 0.0025	+ 0.015	+ 0.006 / - 0.023[c]	
		1.005	+ 0.005[b]	1.013[b]		" "		0.001 - 0.0025		+ 0.012 / - 0.018[c]	
		1.006	+ 0.006[b]	1.011[b]		" "		0.001 - 0.0025		+ 0.009 / - 0.025[c]	
		1.006	+ 0.006[b]	1.012[b]		" "		0.001 - 0.0025		+ 0.010 / - 0.018[c]	
		Not measured				" "		0.001 - 0.0025		+ 0.013 / - 0.013[c]	
		" "				" "		0.001 - 0.003		+ 0.011 / - 0.016[c]	
		1.005	+ 0.005	1.019	18.939	18.999	+ 0.060	0.001 - 0.003		+ 0.010 / - 0.019[c]	+ 0.015 / - 0.012[c]
TT-1	0.9954	0.995	nil	0.997	19.251	19.341	+ 0.090	0.001 - 0.003	- 0.005 / - 0.002[c] / + 0.005	- 0.011 / + 0.019	- 0.006 / + 0.023
TT-3	0.9959	0.996	nil	0.998	19.255	19.344	+ 0.089	0.001 - 0.003			
TT-4	0.9959	0.997	+ 0.001	1.002	19.253	19.303	+ 0.050	0.001 - 0.003		Not measured	
TL-2	0.9996	0.998	- 0.002	0.999	18.935	18.937	+ 0.002	0.001 - 0.002 (Mainly at the upper end)		- 0.012	- 0.011

(a) Accuracy ± 0.001 in. on diameters; ± 0.003 in. on lengths; ± 0.001 in. on bow.
(b) Measured in one plane only.
(c) S shaped.

TABLE 11

FISSION GAS RELEASE

Element	Burn-up[a] (MWd/t U)	$\int_{T_s}^{T_o} k d\theta$ Average (W/cm)	Peak (W/cm)	Fission Product Xenon Formed (ml)	Collected (ml)	Released %	Ratio $\frac{Xe-136}{Xe-134}$
D-29	222	37.2	39.4	11.4	0.28	2.5	-
D-32		37.2	39.4	11.4	0.24	2.1	1.269
D-12		37.2	39.4	11.4	0.08	0.7	-
E-34	282	46.8	49.5	14.4	lost	-	-
E-15		46.8	49.5	14.4	0.17	1.2	-
E-25		46.8	49.5	14.4	0.37	2.6	-
G- 1	521	29.4	34.7	23.0	2.25	9.8	1.277
G- 2	480	29.4	34.7	21.0	lost	-	-
G- 3	535	29.4	34.7	22.8	4.51	19.8	1.272
H- 1	562	36.1	43.9	27.8	3.52	12.6	1.326
H- 2	554	36.1	43.9	27.2	3.66	13.4	1.326
H- 3	554	36.1	43.9	27.4	3.21	11.7	1.326
K- 1	2430	32.4	35.6	12.1	4.81	4.0	1.341
K- 2	2430	32.4	35.6	12.1	5.41	4.2	1.337
J- 1	2520	29.4	32.4	11.1	9.94	9.0	1.329
P- 1	9160	35.2	44.4	46.5	93.1	20.1	1.427
P- 2	9100	35.2	44.4	46.0	123.6	26.8	1.419
P- 3	9090	35.2	44.4	46.0	116.4	25.3	1.426
TT-1	4955	30.0	45.5	26.3	18.0	6.9	1.375
TT-3	4955	30.0	45.5	26.3	21.1	8.0	1.375

(a) Burn-up of bundles D and E estimated from calorimetry; the remainder are derived from chemical analyses. Figures are for 199 MeV/fission.

(b) Based on 182 MeV/fission.

TABLE 12

CONDITION OF THE URANIUM OXIDE AFTER IRRADIATION

Experiment & Element	General Appearance	Ratio of Grain Growth to Pellet Diameter	Cracking	Coalescence of Pellets	Ratio of Void to Pellet Diameter	Remarks
CR-V-k						
D-29	Grain growth was observed in the lower 5 inches of the element. None was observed at the middle or upper end.	Maximum 0.37 at the lower end tapering quickly to zero.	Random; most evident at the lower end.	Slight on one pellet at the lower end. None was observed at the middle or upper end.	None	A few circumferential rings were observed on the end faces of the pellets.
D-32	Fairly extensive grain growth was observed at the lower end but none was seen at the top. Growth region extend- to 12 inches from the bottom.	Maximum 0.52 at the lower end tapering to zero.	Random at the upper end; radial & circumferential at the lower end.	Observed at the lower end where grain growth was prominent. None was seen at the upper end.	None	Same as for D-29.
D-12	Grain growth had occurred in the lower 8 inches of the element. No growth was seen in the upper portion	Maximum 0.52 at the lower end tapering quickly to zero.	Random at the upper end; radial and circumferential at the lower end.	Slight in the lower sections where grain growth was observed. There was none at the upper end.	None	Same as for D-29.
E-34	Grain growth was apparent along the length of the element. Columnar grains were seen at the lower end.	At the upper end 0.46; at the lower end 0.43; average 0.35.	Radial and circumferential.	Observed at all of six pellet ends examined.	Indication at lower end.	Same as for D-29.
E-15	Grain growth was apparent along the length of the element with columnar grains occurring at the top and bottom.	At the upper end 0.52; at the lower end 0.42; average 0.34.	Radial and circumferential.	Observed at the upper end of the element. At the middle & lower end the pellet faces appeared flat.	Indication near the upper end.	Same as for D-29.

TABLE 12 CONT'D

CONDITION OF THE URANIUM OXIDE AFTER IRRADIATION

Experiment & Element	General Appearance	Ratio of Grain Growth to Pellet Diameter	Cracking	Coalescence of Pellets	Ratio of Void to Pellet Diameter	Remarks
E-25	Grain growth was apparent along the length of the element. Columnar grains radiated from a void near the bottom	At the upper end 0.56; at the lower end 0.59; average 0.41.	Radial and circumferential.	Prominent near the lower end. Slight near the upper end. The remainder of the pellet faces appeared flat.	At the lower end.	Same as for D-29
CR-V-m						
G- 1	Equiaxed and columnar grain growth was observed along the length of each element. The diameter of the growth region tapered toward the low flux end, then increased at the end.	Average 0.32	Radial and circumferential.	Observed over a large portion of the grain growth area.	None	
G- 2		Average 0.36	Radial and circumferential.	Same as for G-1.	At the high flux end 0.03 maximum	
G- 3		Average 0.42	Radial and circumferential.	Same as for G-1.	At the high flux end and intermittently along the element; 0.06 maximum.	
H- 1	Equiaxed and columnar grain growth was observed along the length of the elements	Average 0.45	Radial and circumferential.	Same as for G-1.	At the ends and intermittently along the length 0.06 max.	Coalescence occurred even though the pellet ends were dished. A deposit was observed on the shoulder of the dishing as shown in Figure 9.
H- 2		Average 0.52	Radial and circumferential.	Same as for G-1.	At the ends and intermittently along the length 0.11 max.	
H- 3		Average 0.54	Radial and circumferential.	Same as for G-1.	At the ends and intermittently along the length 0.05 max.	
CR-V-n						
K- 1	Grain growth was observed along the length of the element with equiaxed & columnar growth at the lower end.	Maximum 0.54 Average 0.32 Minimum 0.19	Radial and circumferential.	Slight at the upper end and over the grain growth area at the lower end.	Very small void at the lower end; 0.02 maximum.	There were concentric rings on the ends of the pellets. This appeared to be a surface effect and did not extend into the interior of the pellet.
K- 2	Grain growth was observed at the ends of the element; greatest growth was at the lower end.	Maximum 0.49 Average 0.32 Minimum Nil	Radial and circumferential.	Observed at the lower end in the grain growth area.	At the lower end there was possibly a small void.	

TABLE 12 CONT'D

CONDITION OF THE URANIUM OXIDE AFTER IRRADIATION

Experiment & Element	General Appearance	Ratio of Grain Growth to Pellet Diameter	Cracking	Coalescence of Pellets	Ratio of Void to Pellet Diameter	Remarks
J- 1	Grain growth was observed at the upper end and in the lower 3/4 of the element.	Maximum 0.64 Average 0.40 Minimum Nil	Radial and circumferential	Observed at the lower and upper ends over the grain growth area.	At the upper end 0.06 maximum. At the lower end 0.05 maximum.	Same as for K-1 and K-2.
X-5-o						
P- 1	Grain growth was observed along the length of the elements as shown in Fig. 10, 11 and 12. The growth was least around the mid planes and greatest at the upper end. Columnar growth had occurred at the ends but elsewhere there were large equiaxed grains. Broken oxide surfaces exhibited more growth than the pellet end faces.	At the upper end 0.68. At the middle 0.52. At the lower end 0.61.	The grain growth region was less fractured than the outer edge of the pellets and was separated from it by a circumferential crack. Radial cracking predominated especially when columnar growth was present but at the pellet edges & in regions of equiaxed growth circumferential and random cracking was also visible.	Observed in the grain growth region at many of the pellet interfaces especially the upper end.	At the upper end in the first and second pellets; 0.22 max.	The voids in elements P-1 and P-2 contained a cluster of triangular faces crystals (Fig.13). Some of the equiaxed grains in P-2 and P-3 were elongated in the direction of the pellet radii to form a transitional structure bearing resemblance to both columnar & equiaxed growth. White particles observed in grain growth area (Fig.14).
P- 2		At the upper end 0.79. At the middle 0.64. At the lower end 0.74.		Observed in the grain growth region at most of the pellet interfaces.	At the upper end in the first, second and third pellets; 0.33 maximum.	
P- 3		At the upper end 0.71. At the middle 0.63. At the lower end 0.68.		Observed in the grain growth region at most of the pellet interfaces.	At the upper end in the first & second pellets; 0.30 max.	
TT-1	Some equiaxed grain growth was observed along the length of the original three elements (Fig.15) No columnar growth or void was evident. In general growth was greatest at the lower end & least around the mid plane of the elements. Broken oxide surfaces exhibited more growth than the pellet end faces.	At the upper end 0.33. At the middle 0.35. At the lower end 0.42.	Generally the grain growth region was less fractured than the outer edge of the pellets. The two regions were separated by a circumferential crack. Radial cracking predominated but some pellets were extensively fractured in a random manner	Observed in the grain growth region at some of the pellet interfaces.	None	White particles observed in grain growth boundaries in grain growth region of TT-1 and TT-3 (Fig.16).
TT-3		At the upper end 0.44. At the middle 0.35. At the lower end 0.51.		Same as for TT-1.	None	
TT-4		At the upper end 0.31. At the middle 0.25. At the lower end 0.38.		Same as for TT-1.	None	Outer oxide separated at grain boundaries as shown in Fig.17.
TL-2	The replacement element had equiaxed grain growth at the upper end only.	At the upper end 0.31.	Random	Observed in the grain growth region.	None	

TABLE 13

METALLOGRAPHIC EXAMINATION OF SHEATHS

Bundle & Element	ZrO_2 film on outer surface	ZrO_2 film on inner surface	ZrO_2 film in fuel/ end cap interface	ZrH_2 distribution in sheath	Orientation of ZrH_2 platelets in sheath	ZrH_2 distribution in end cap	ZrH_2 distribution in end plate
K-2	uniform film 4 μm thick	not detected	not examined	higher concentration at outer surfaces (Fig.21). Sections from bottom had less H_2 than those taken near top.	random at outer surface, mainly parallel to sheath surface at mid-sheath and inner surface.		
TT-1 TT-3	discontinuous film about 2 μm thick (Fig.22a)	discontinuous film average thickness of 3 μm (Fig.22b)	discontinuous film 3 μm thick (Fig.22c)	higher at outer surfaces	mainly parallel to sheath surfaces (Fig.23)	hydride content low at fuel/cap interface. Concentration increased at shoulders & was highest in the spigot.	
TL-2	film about 2 μm thick	film up to 3 μm thick	discontinuous film up to 3 μm thick	uniform distribution	mainly parallel to sheath surface	as for TT-1 and TT-3	
P-1 P-2 P-3	discontinuous film, average thickness of 3 μm. Minimum thickness 1.5 μm and maximum 5 μm.	discontinuous film up to 3 μm thick	discontinuous film with average thickness of 4 μm	much higher concentration at outer surfaces. One quarter of sheath had lower content compared to remainder of sheath (Fig. 24 a & b)	Widmanstätten structure (Fig.24)	similar distribution as TT-1. In the spigot numerous large platelets were distributed at the grain boundaries, with much finer precipitate within the grains (Fig.25)	plateletts were oriented parallel to faces of end plate. (Fig.25)

TABLE 14

TRANSVERSE TENSILE TEST RESULTS

Specimen	Proportional Limit (k psi)	Ultimate Tensile Strength (k psi)	Relative Ductility
TT archive	62.3	75.1	High-extensive elongation - cup and cone fracture.
P archive room temperature	52.5	67.8	Visible necking in gauge length.
TT-1 and TT-3 room temperature	89	97	Low
TL-2	71.5	81.5	Moderate to high.
P-1, P-2, P-3 room temperature	46.1 to 88.4 Avg. 74.4	46.1 to 95.6 Avg. 84.1	Very low; some showed no ductility.
P-1, P-2, P-3 at 280°C	47	53	Very low.

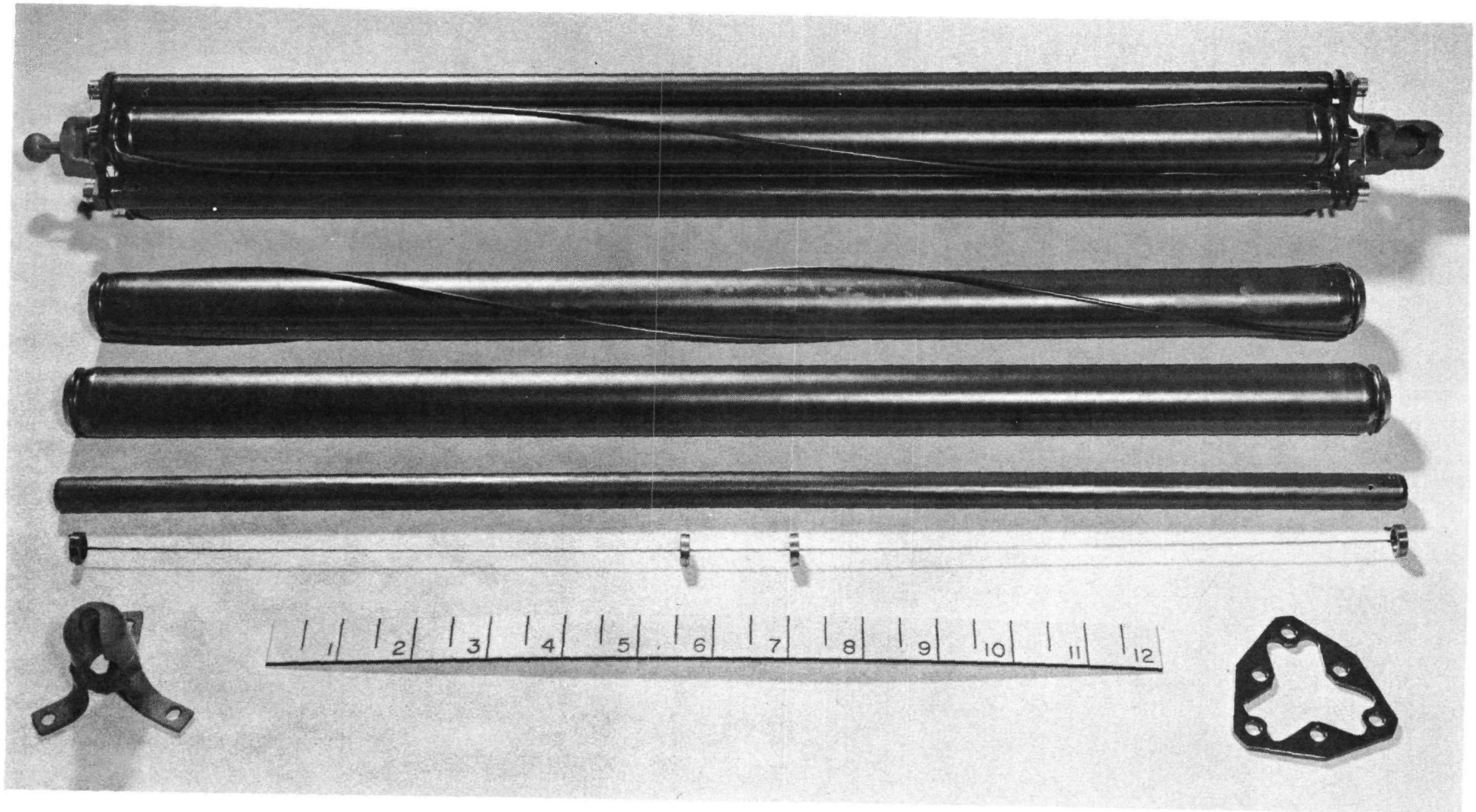

Fig. 1 Assembled bundle, elements and spacer rods for Trefoil Irradiations.

Photo 1630-5

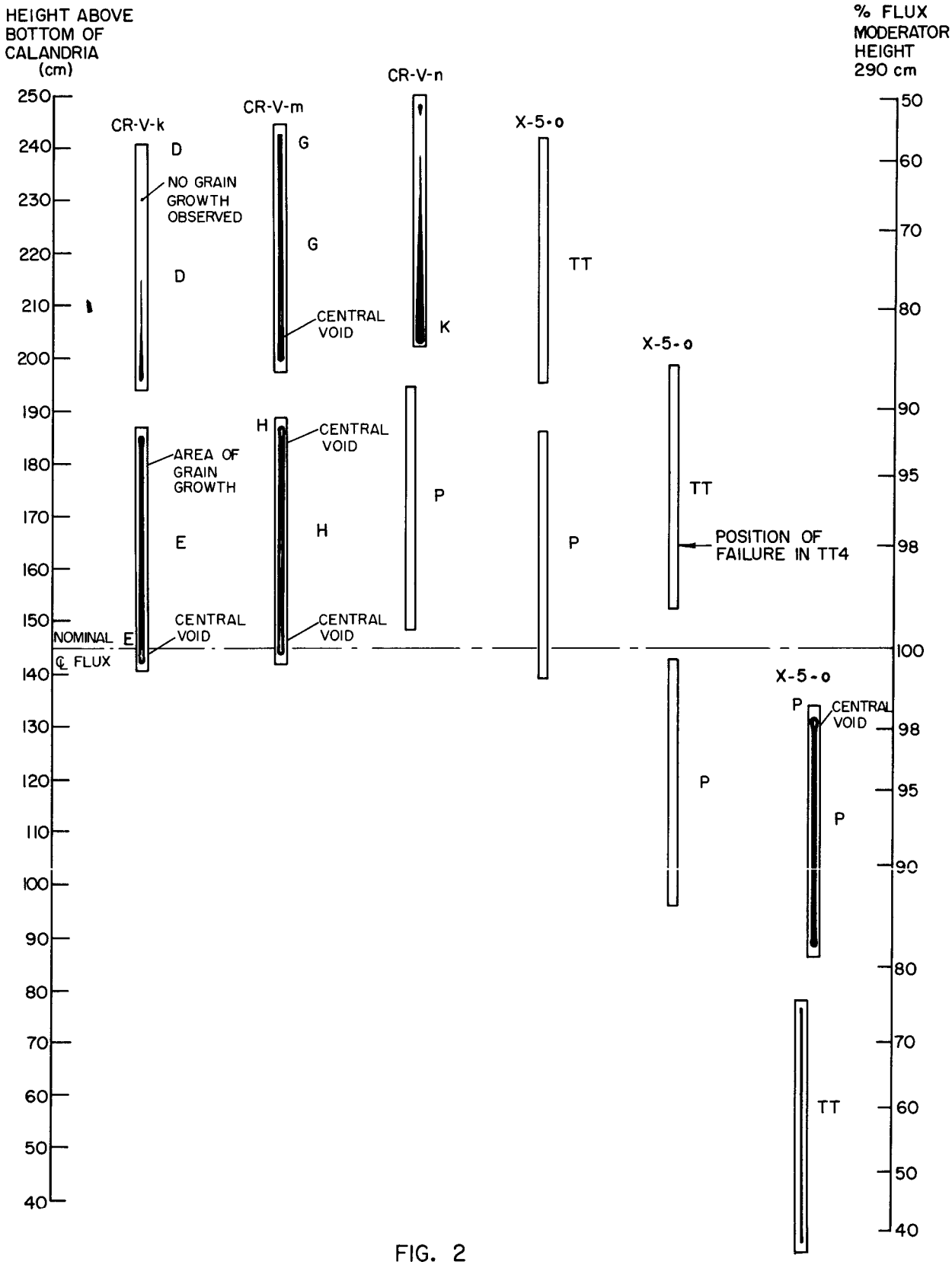

FIG. 2

POSITION OF FUEL BUNDLES DURING IRRADIATION SHOWING EXTENT OF GRAIN GROWTH

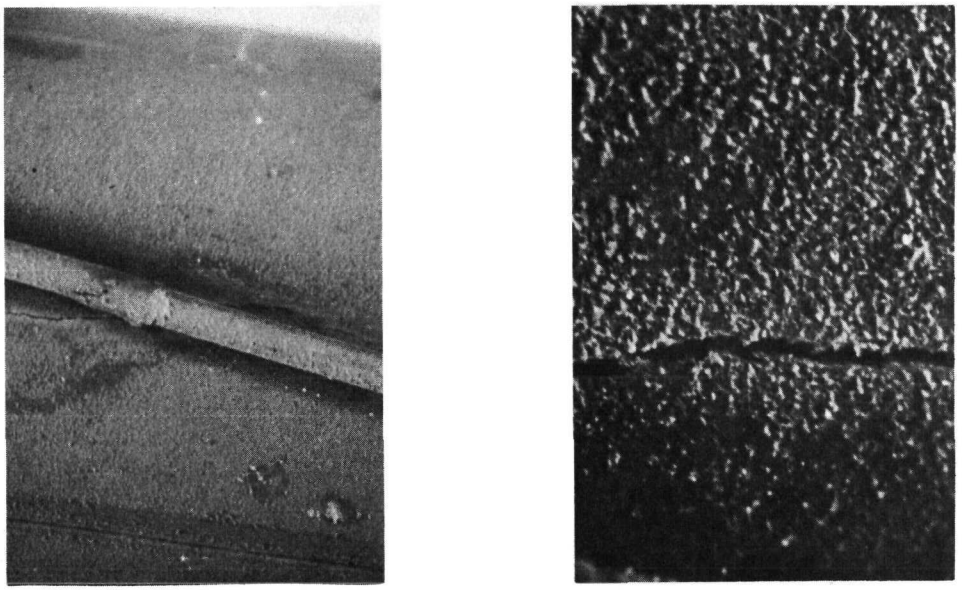

(a) (b)

Fig. 3 Split in sheath of TT-4 passing near wire wrap weld. Note brittle type of failure.

References (a) 5870 4 X
(b) 5871 30 X

FIGURE 4 POST IRRADIATION DIAMETER TRACES ON ELEMENTS FROM BUNDLE P

EXP NRX 3100

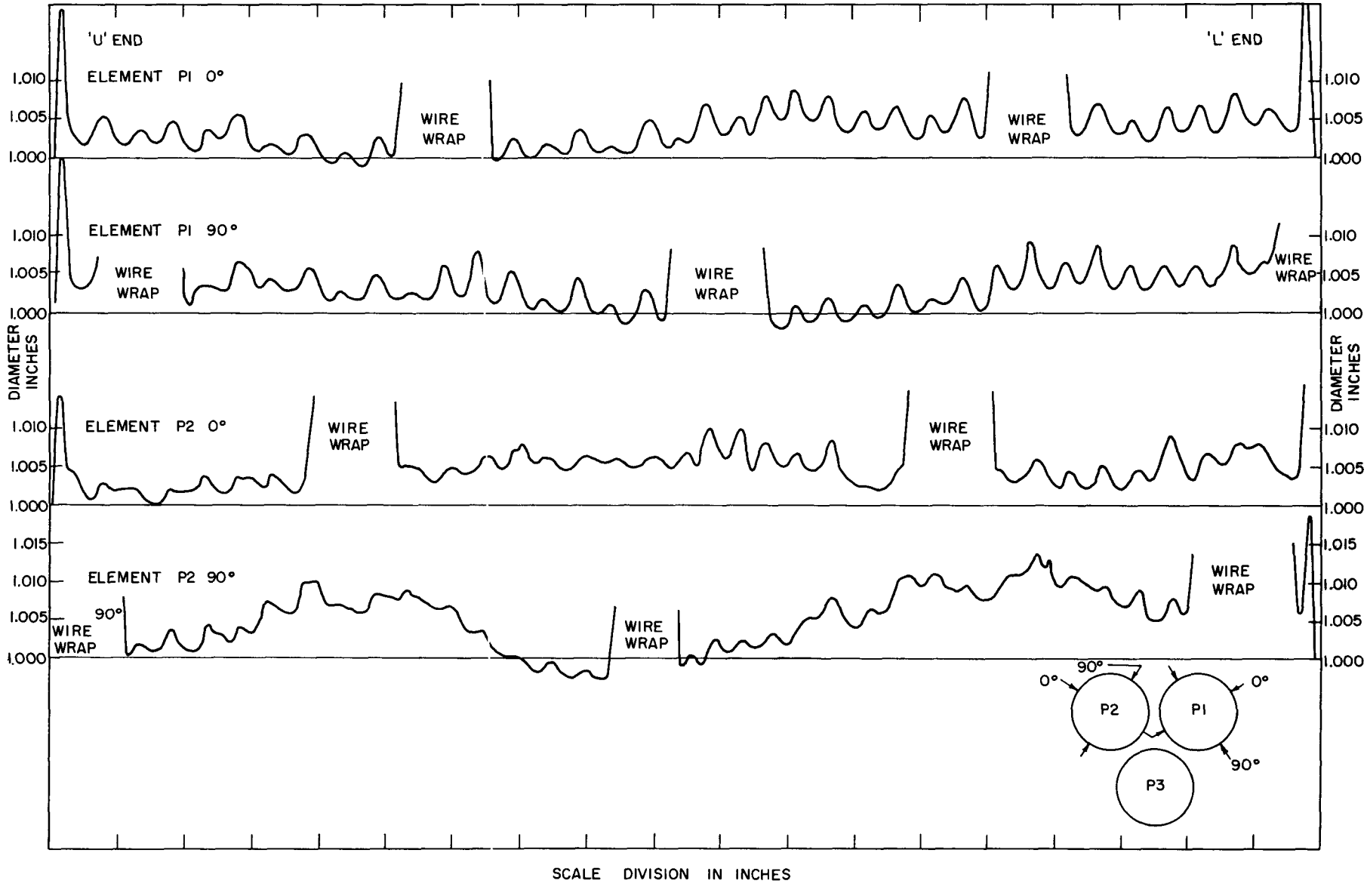

SCALE DIVISION IN INCHES

FIGURE 5 POST IRRADIATION DIAMETER TRACES ON ELEMENT P3 EXP NRX 3100

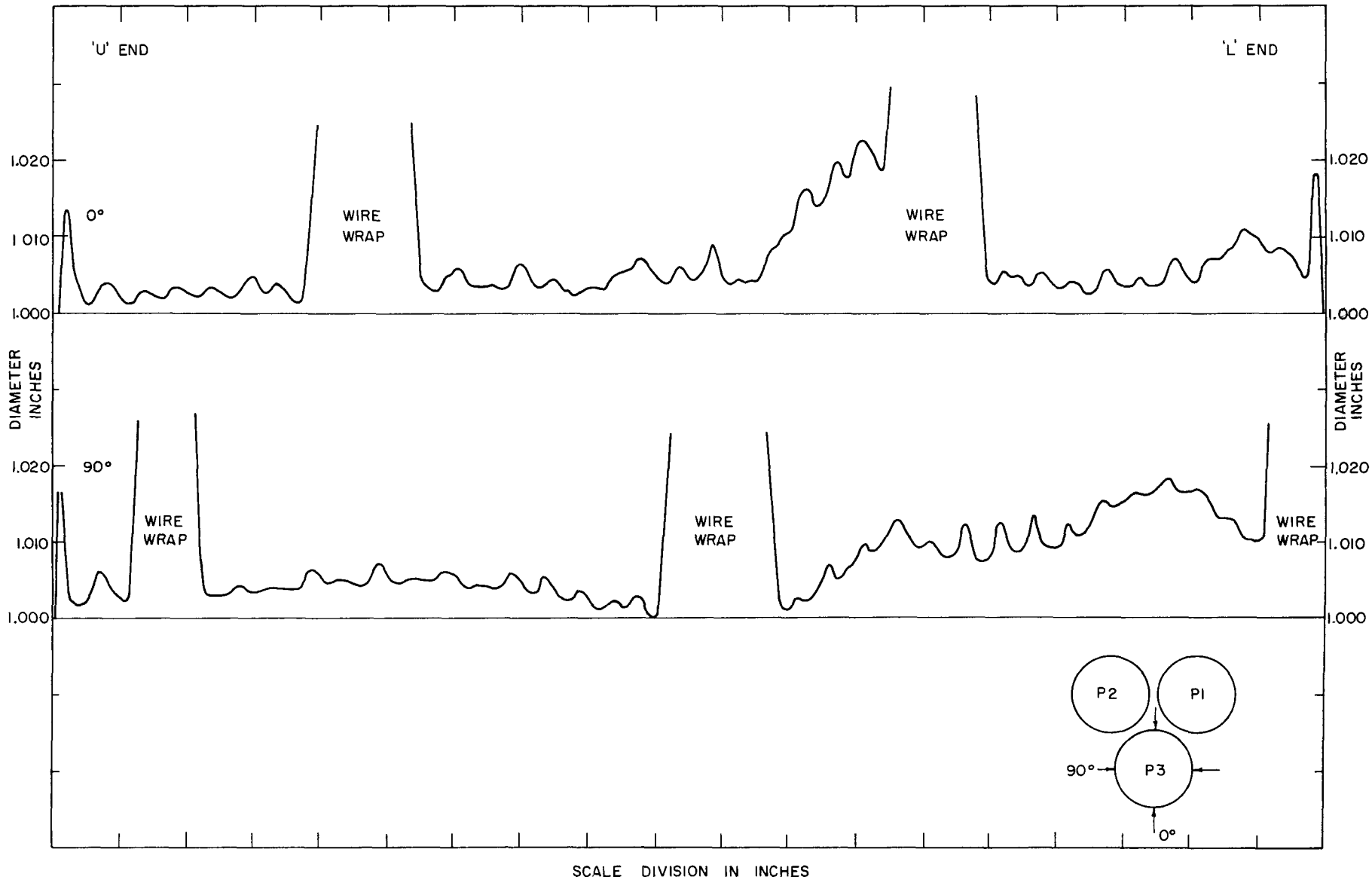

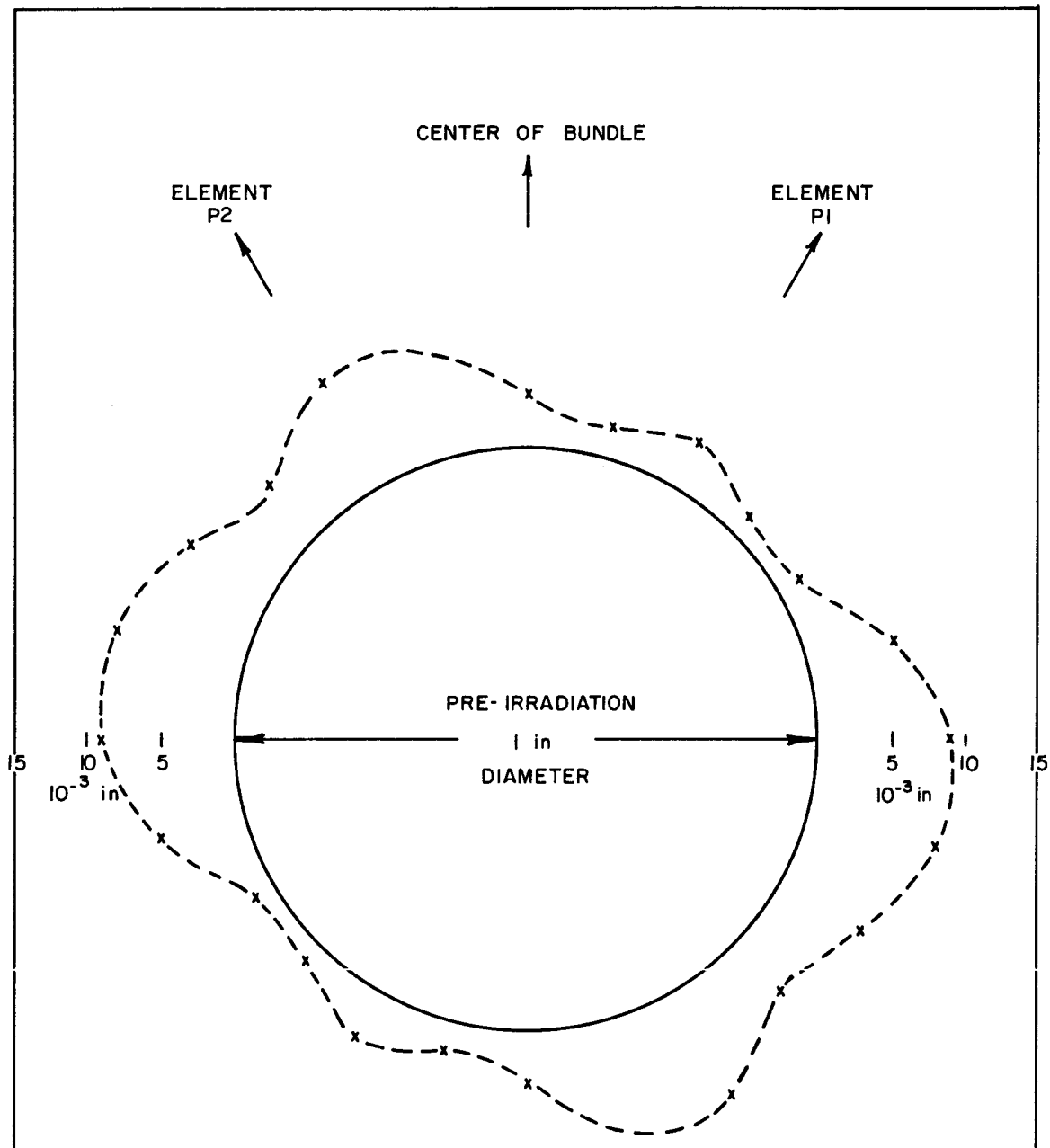

FIG. 6a ELEMENT P3 DIAMETER AT 2 in FROM 'L' END

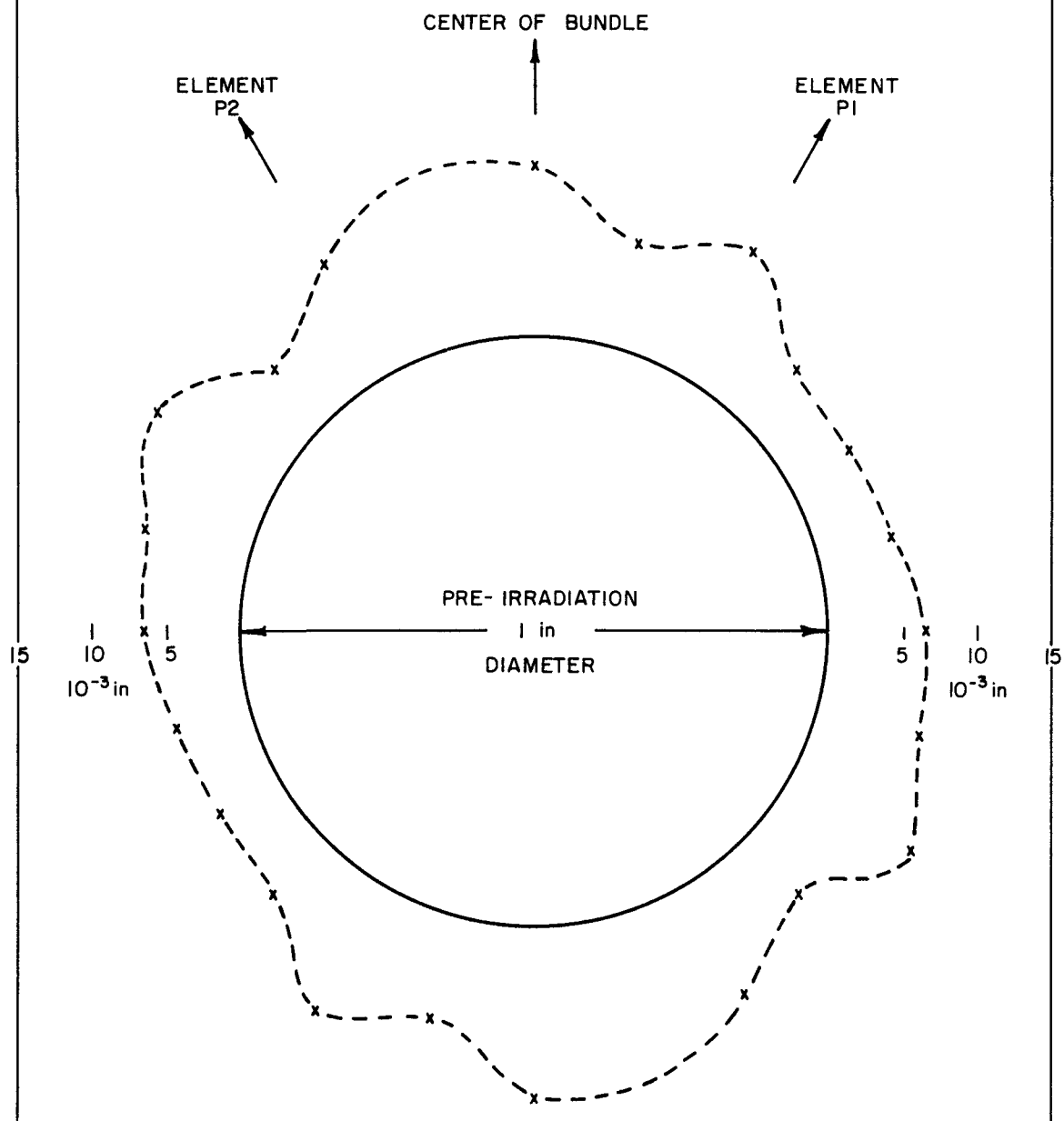

FIG. 6b ELEMENT P3 DIAMETER AT $6\frac{1}{2}$ in FROM 'L' END

FIGURE 7 PROFILE TRACES ON BUNDLE P ELEMENT P1 EXP. NRX 3100

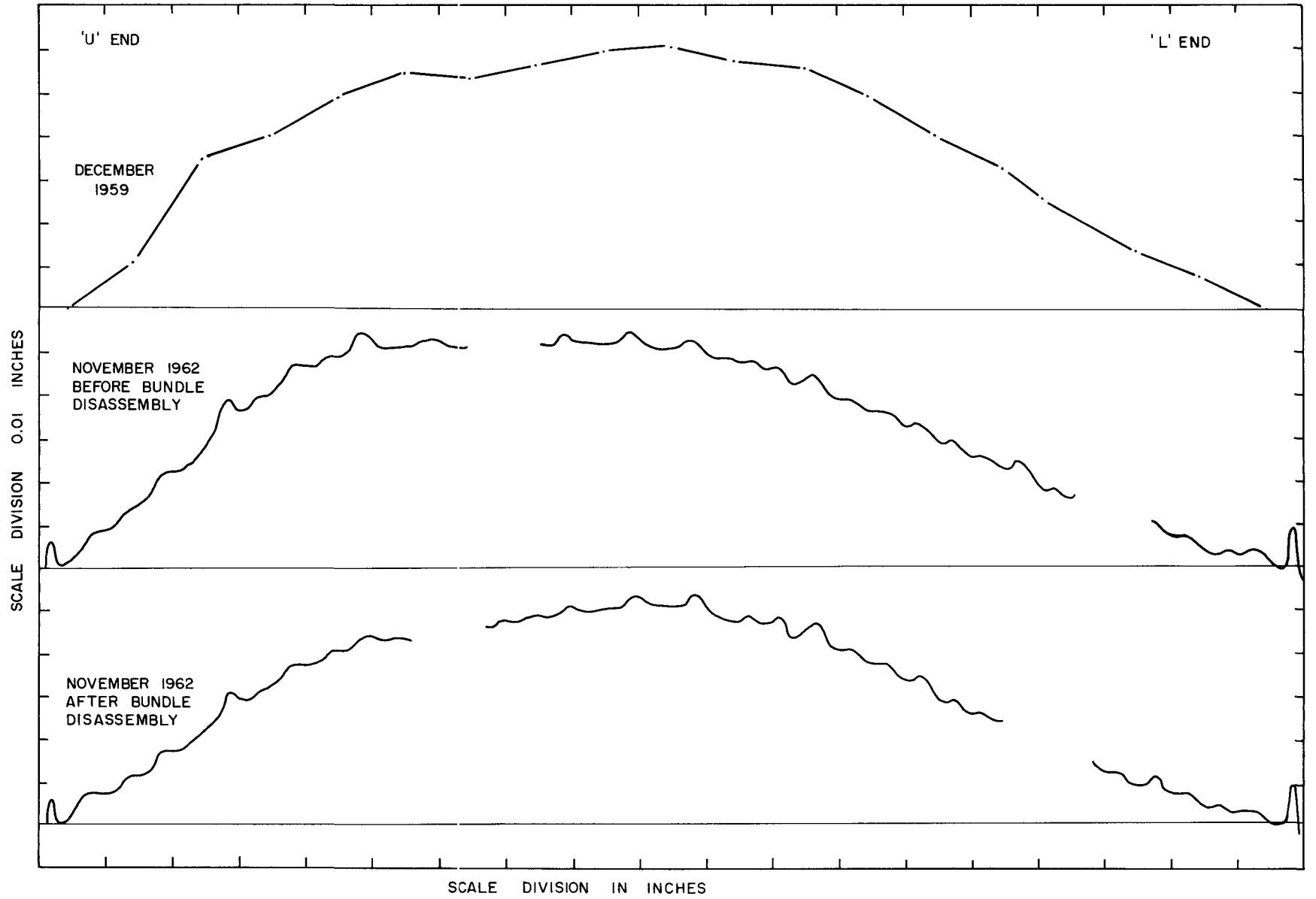

FIGURE 8 PROFILE TRACES ON BUNDLE P ELEMENT P3 EXP NRX 3100

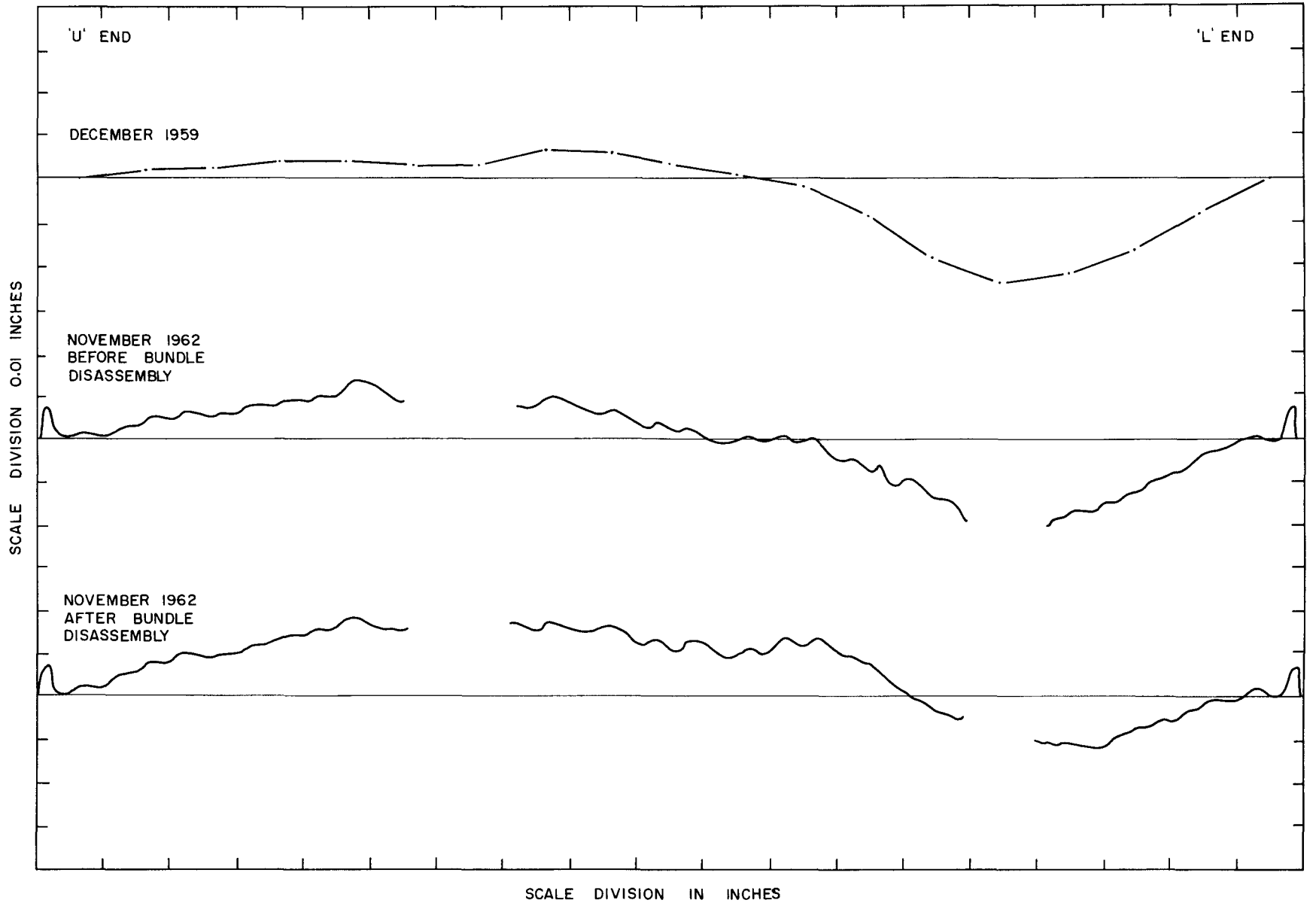

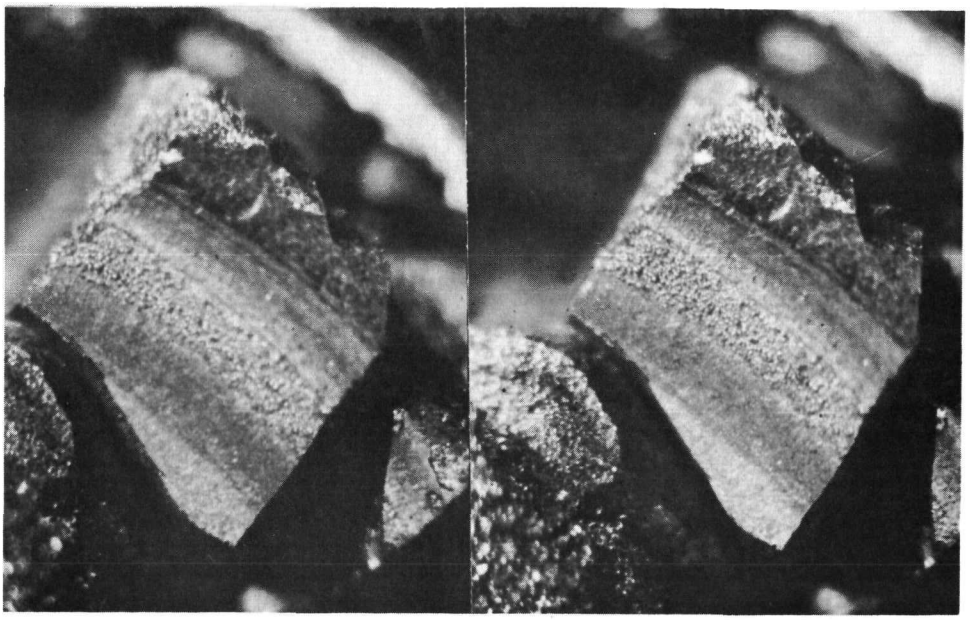

Fig. 9 Deposit on shoulder of pellet end dishing in bundle H.

Reference 2354 12 X

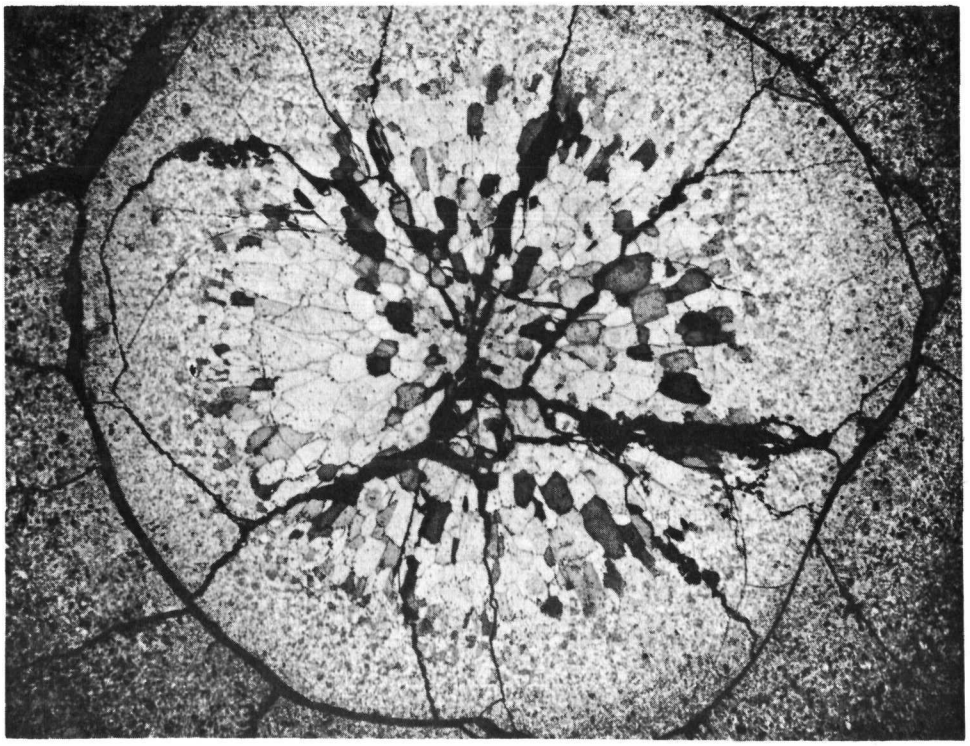

Fig. 10 Equi-axed grain growth in UO_2 from bundle P.

Reference X2-C1 7.5 X

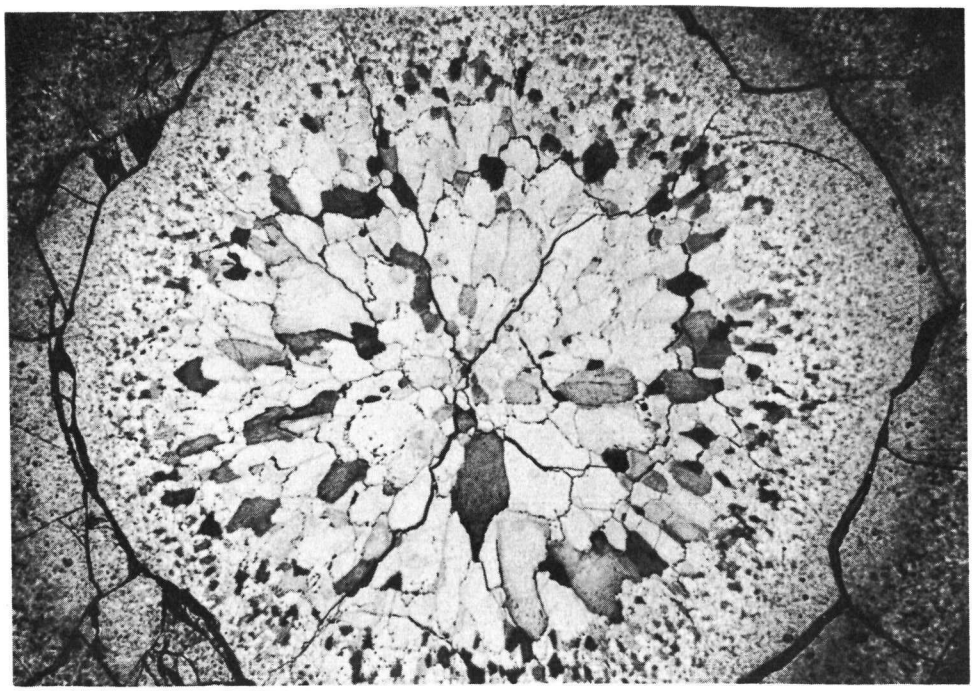

Fig. 11 Very large equi-axed and broad columnar grains in UO_2 from bundle P.

Reference X2-E1 7.5 X

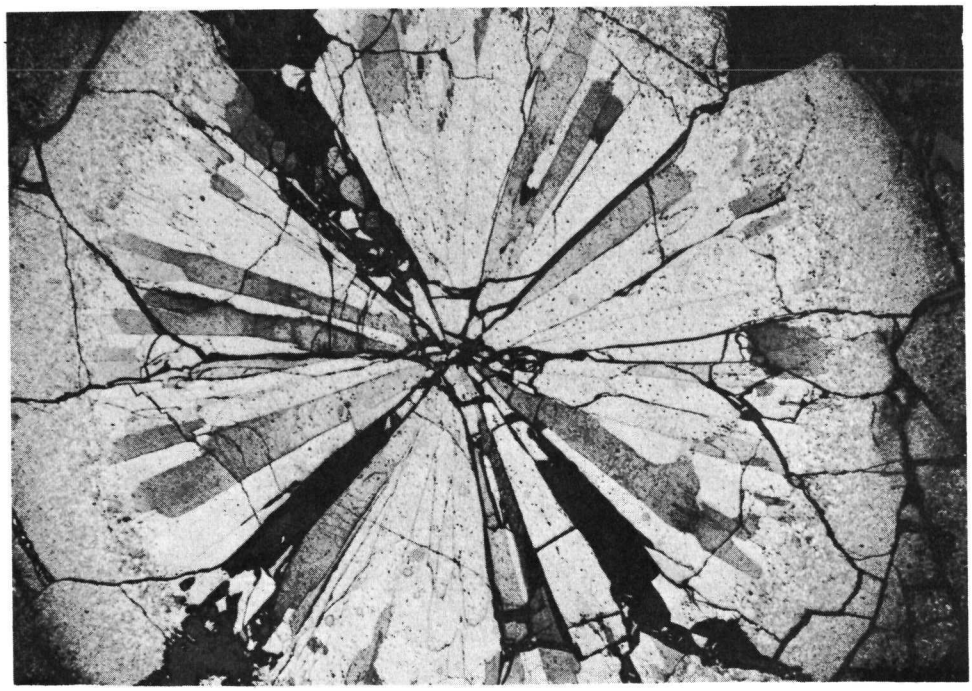

Fig. 12 Long columnar grains found in UO_2 near lower end of bundle P.

Reference X2-F1 7.5 X

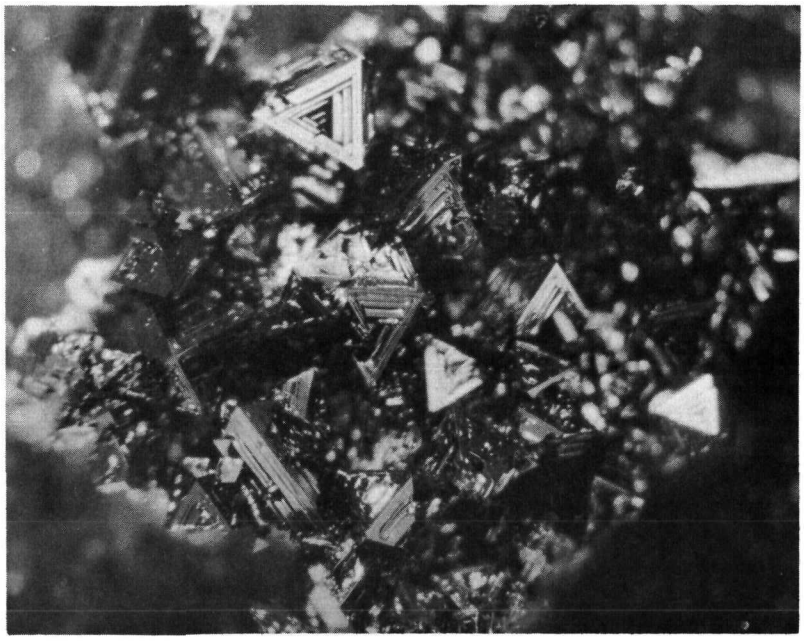

Fig. 13 Vapour deposit found in central void of element P-2.

Reference 7491 50 X

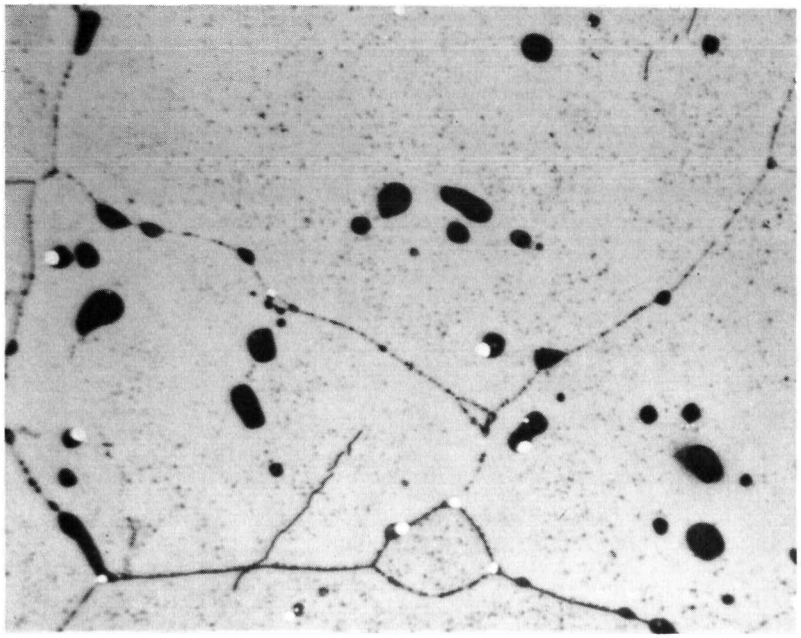

Fig. 14 White particles in irradiated UO_2 from bundle P.

Reference X2-E2 500 X

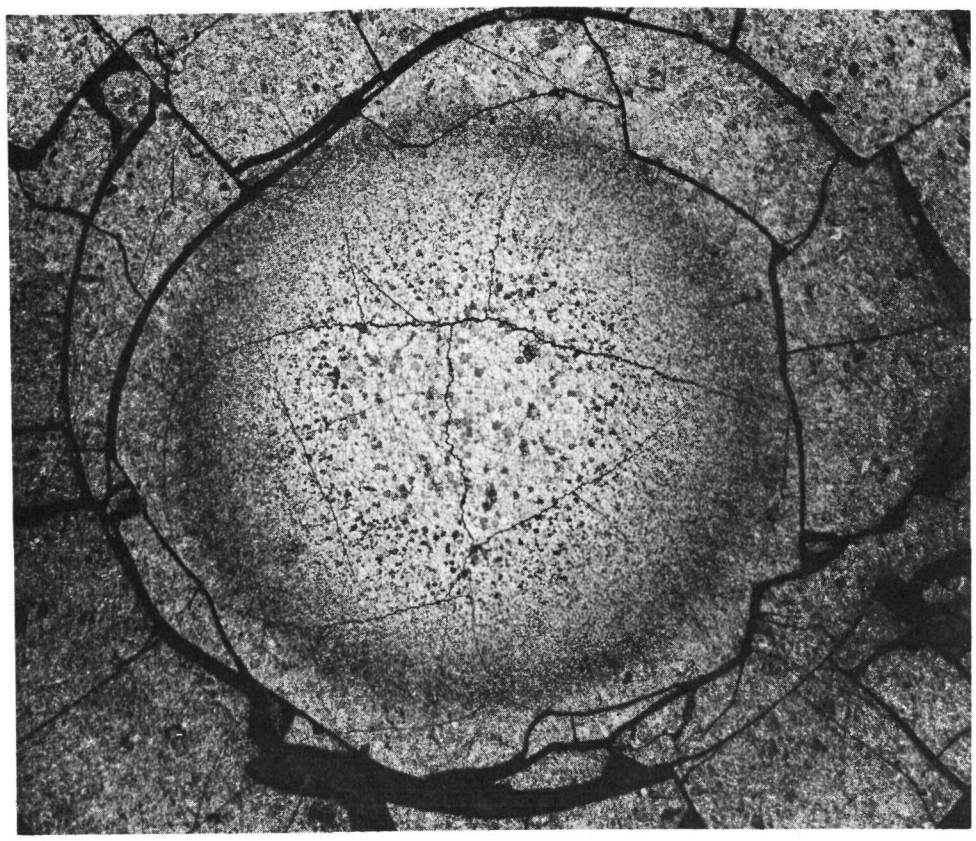

Fig. 15 Small equi-axed grain growth of UO_2 in bundle TT.

Reference Y-82-D1 7.5 X

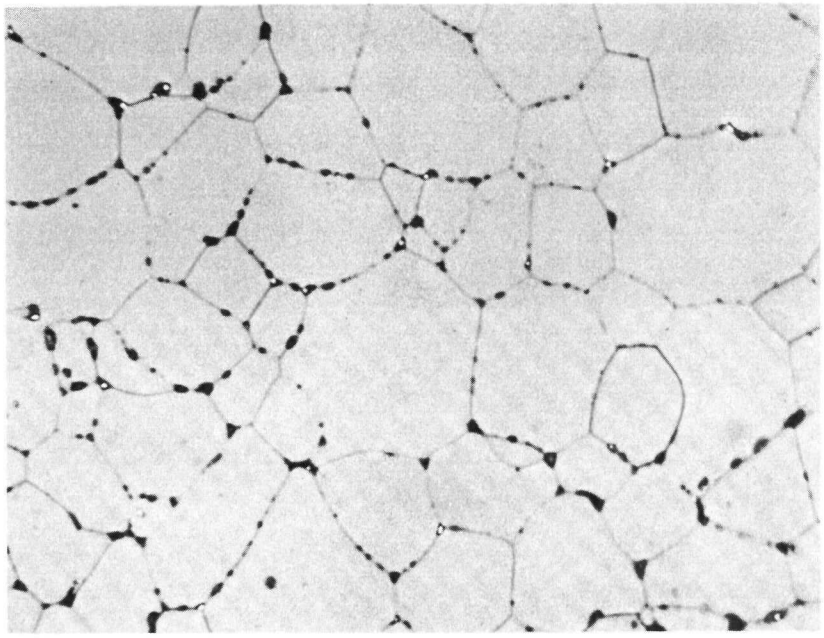

Fig. 16 Small amount of white deposit in grain boundaries of UO_2 from bundle TT.

Reference Y-82-A1 500 X

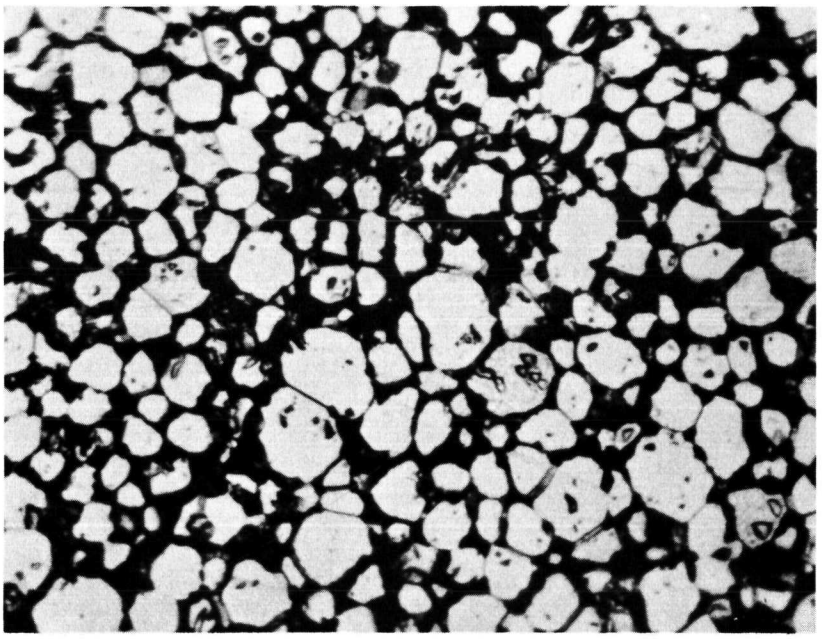

Fig. 17 Separation of individual grains of UO_2 in outer regions of element TT-4.

Reference Y-10-A3 500 X

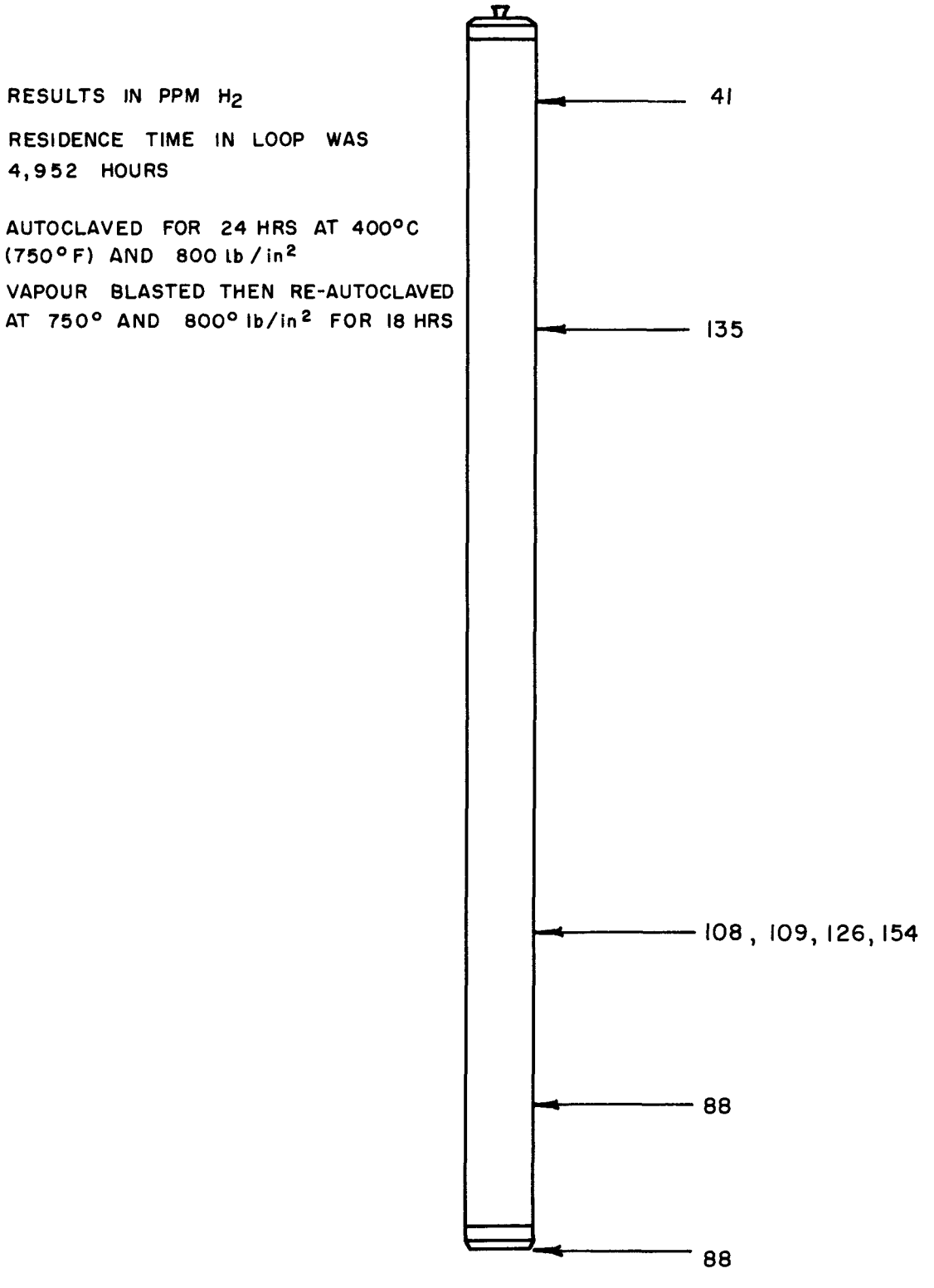

FIG. 18

HYDROGEN CONTENT IN ELEMENT K-2 OF CR-V-n

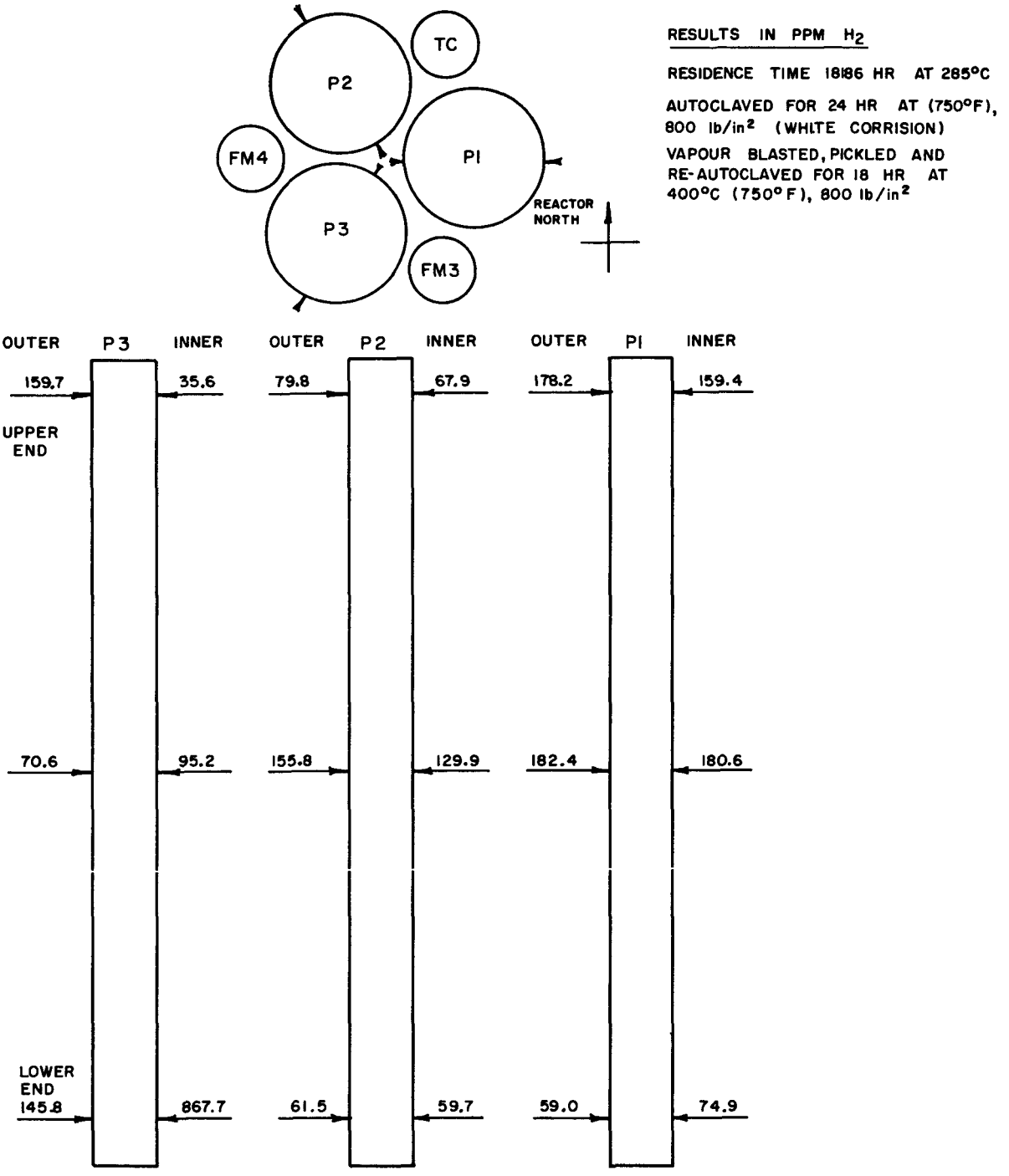

FIG. 19

HYDROGEN CONTENT IN BUNDLE P OF X-5-o

RESULTS IN PPM H_2

RESIDENCE TIME IN REACTOR AT 285°C

TT1	12055 HOURS
TT3	12055 "
TT4	10861 "
TL2	1194 "

AUTOCLAVE TIME AT 400°C (750°F), 800 DROPPING TO 500 lb/in^2

TT1, TT2, & TT4 72 HOURS

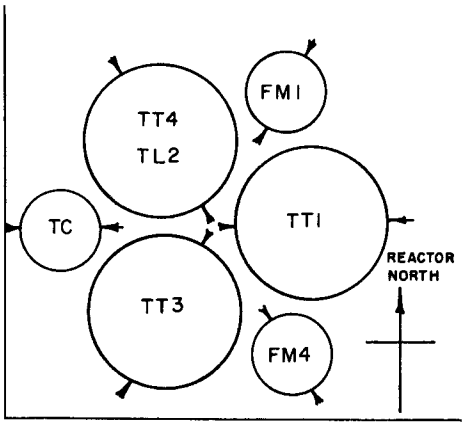

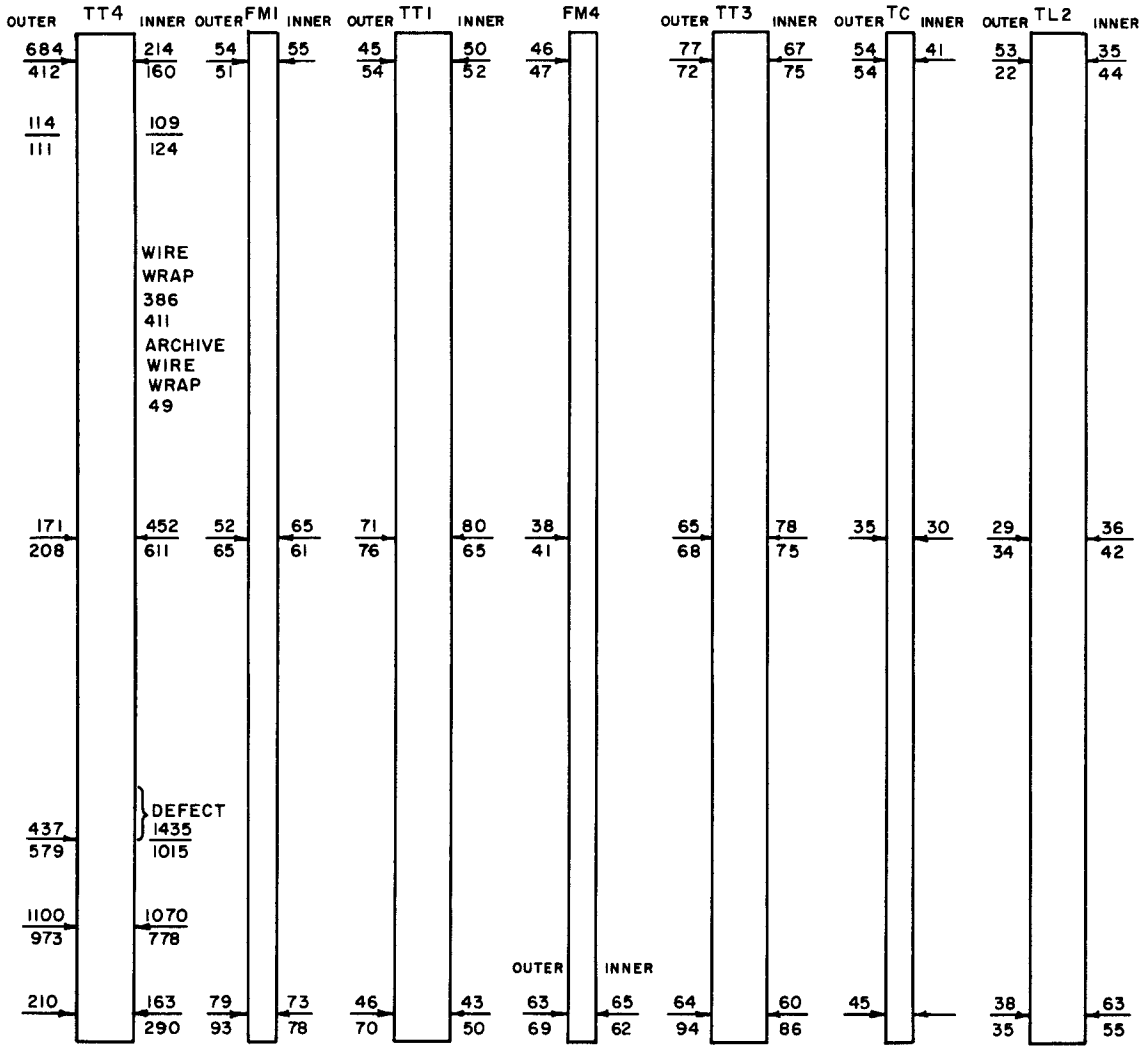

FIG. 20

HYDROGEN CONTENT OF BUNDLE TT OF X-5-o

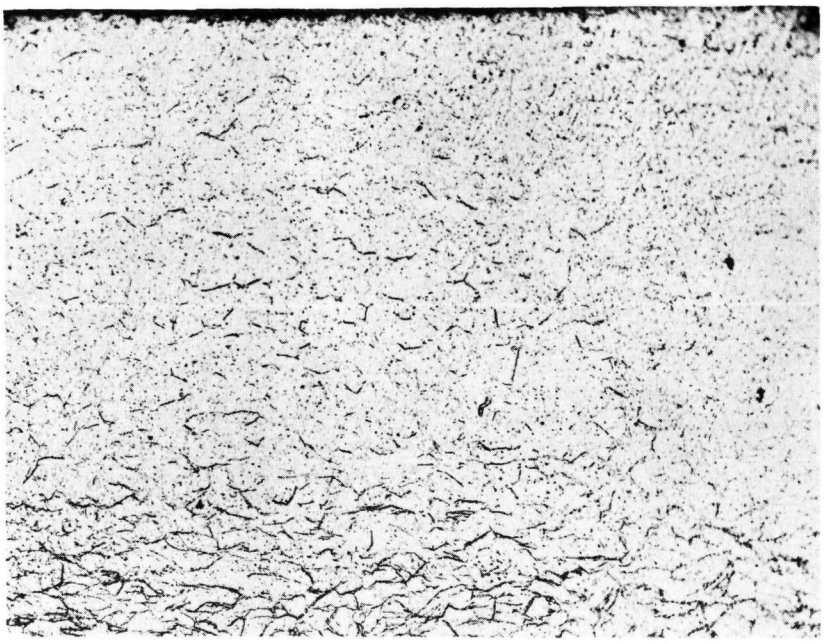

Fig. 21 ZrH_2 precipitation in sheath of element K-2 showing higher concentration at outer surface.

Reference Z8-A1 100 X

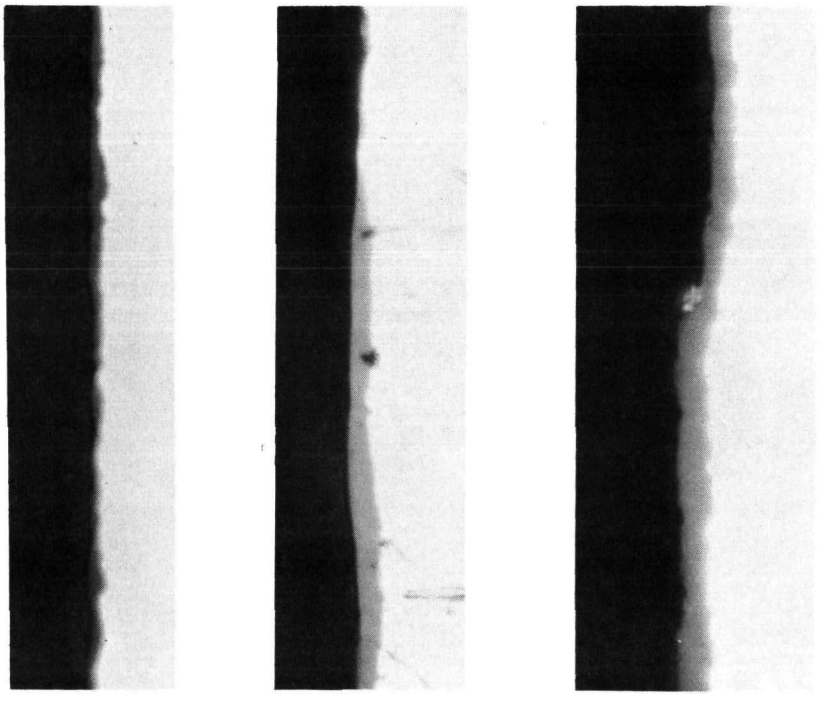

(a) (b) (c)

Fig. 22 Zirconium oxide films on inner (a) and outer (b) surfaces of sheath and on UO_2/end cap interface (c) of bundle TT.

(a) Y-83-A1 (b) Y-83-F1 (c) Y-82-B1 1000 X

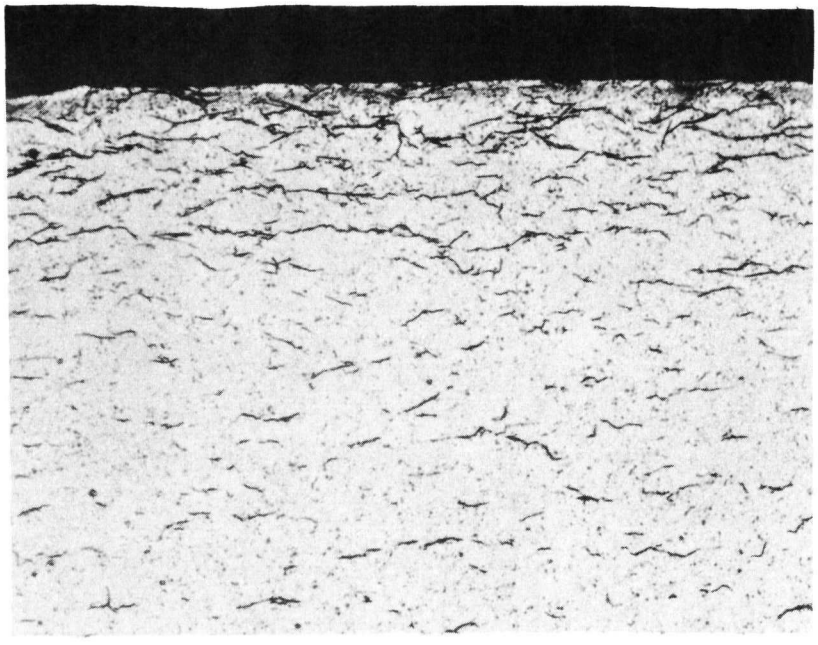

Fig. 23 Precipitation of ZrH_2 parallel to surface of sheathing from bundle TT.

Reference Y-83 -B2 250 X

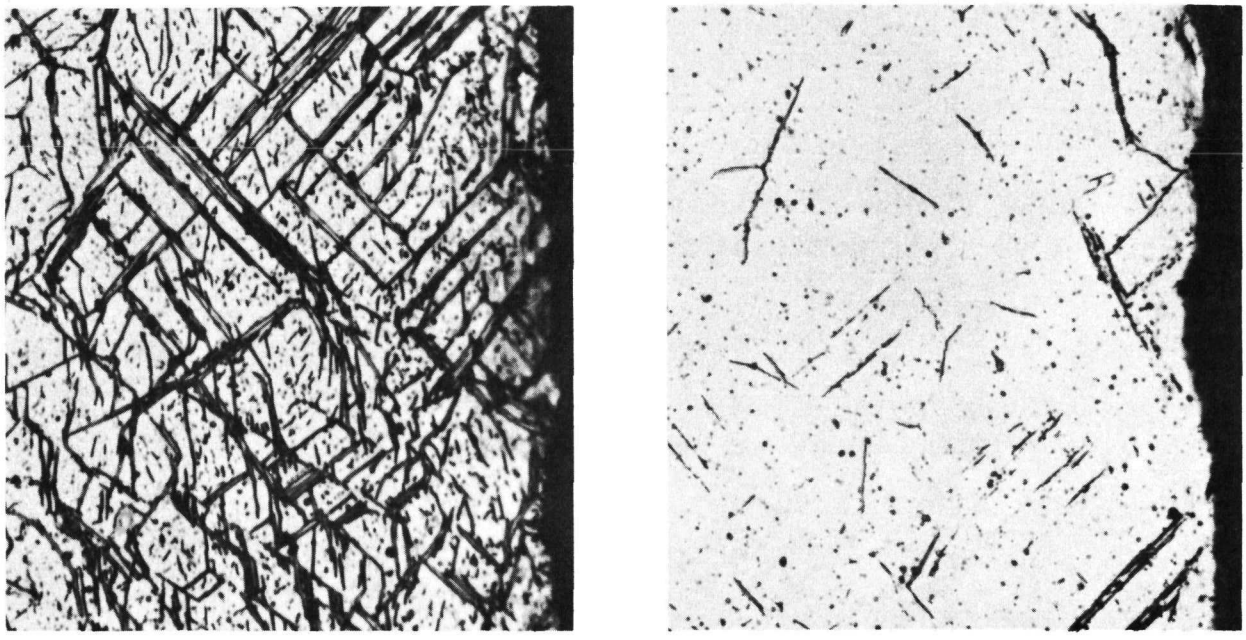

(a) (b)

Fig. 24 Widmanstätten - like precipitation of ZrH_2 at outer surface of sheathing of bundle P. Lower concentration was observed in one quarter of the circumference only.

(a) X2-B2 (b) X2-B4 500 X

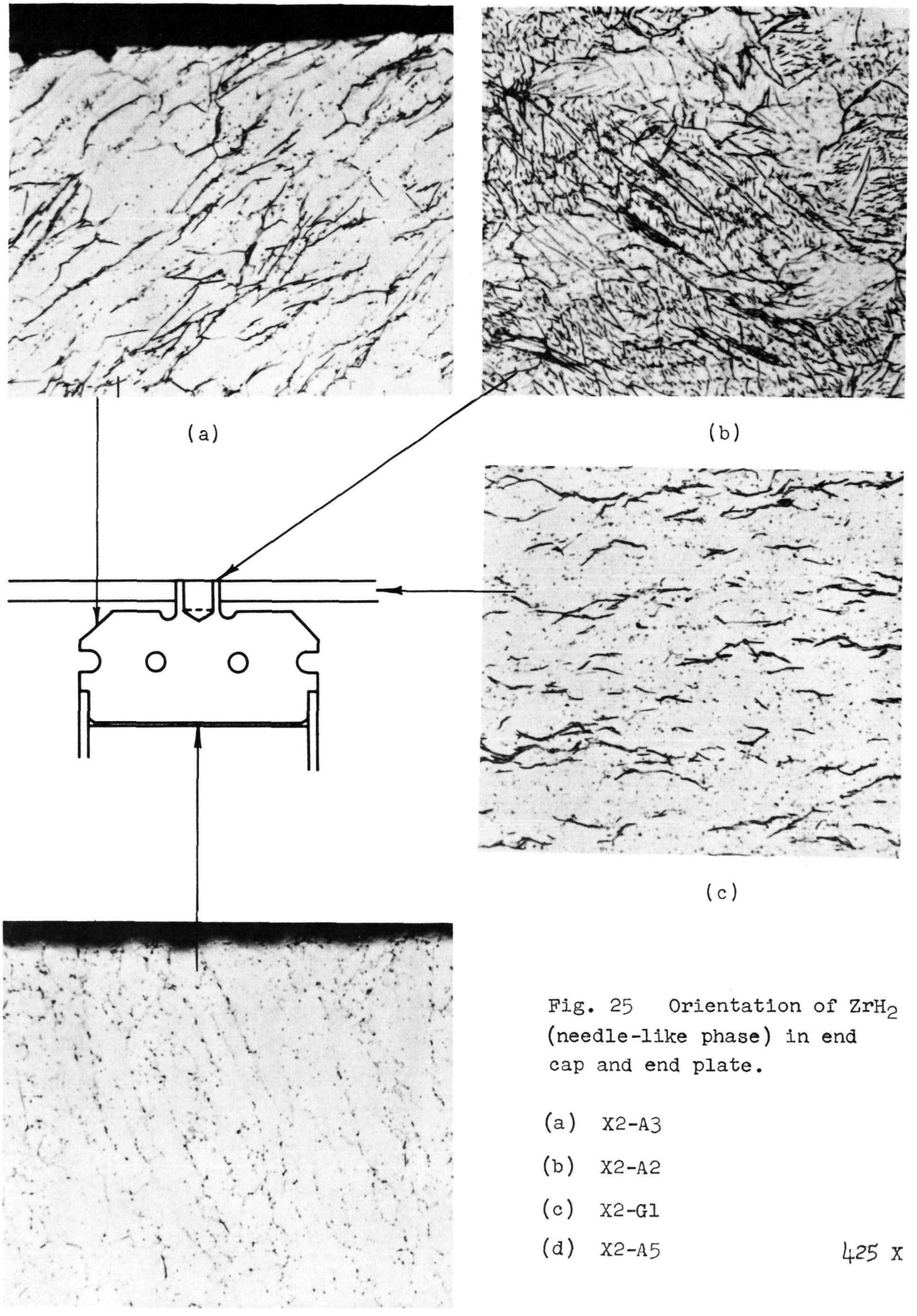

Fig. 25 Orientation of ZrH_2 (needle-like phase) in end cap and end plate.

(a) X2-A3

(b) X2-A2

(c) X2-G1

(d) X2-A5 425 X

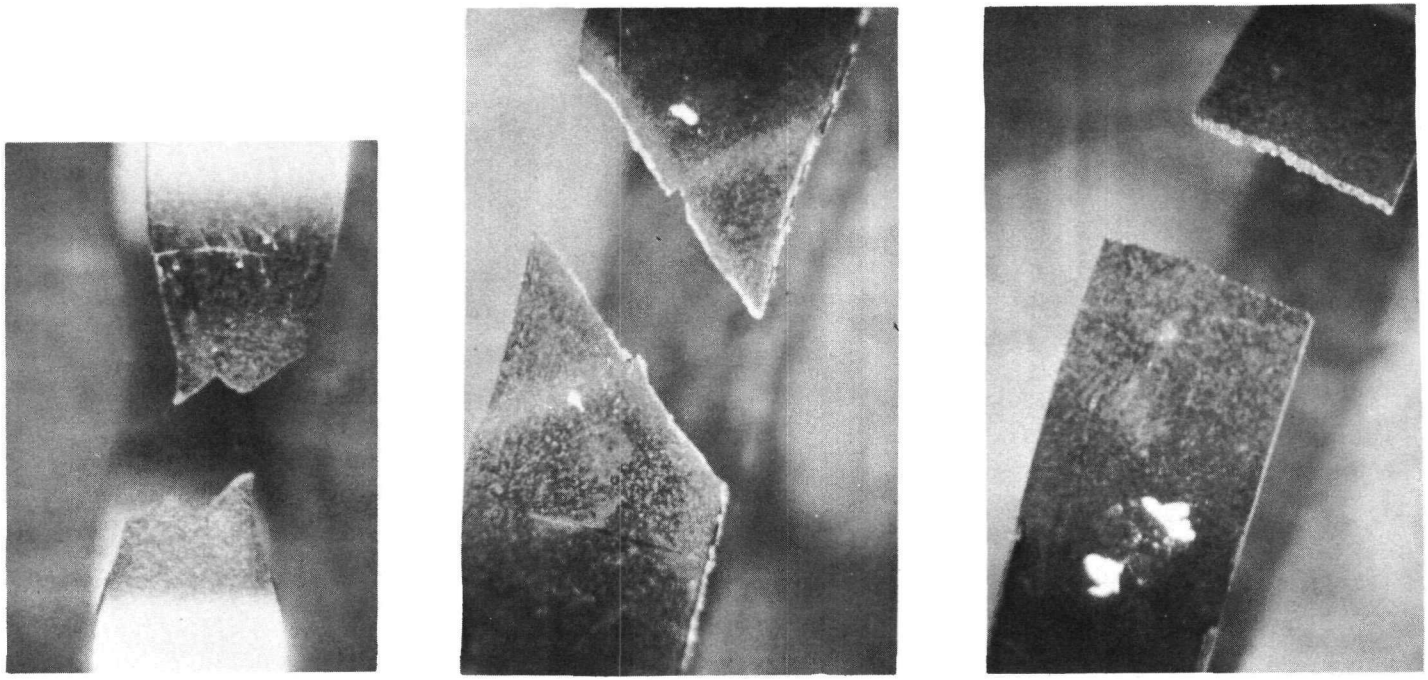

(a) (b) (c)

Fig. 26 Type of fracture in room temperature ring tensile tests.
(a) unirradiated material from bundle TT (7699)
(b) irradiated ring from TT-1 (7696)
(c) irradiated ring from P-2 (7698)

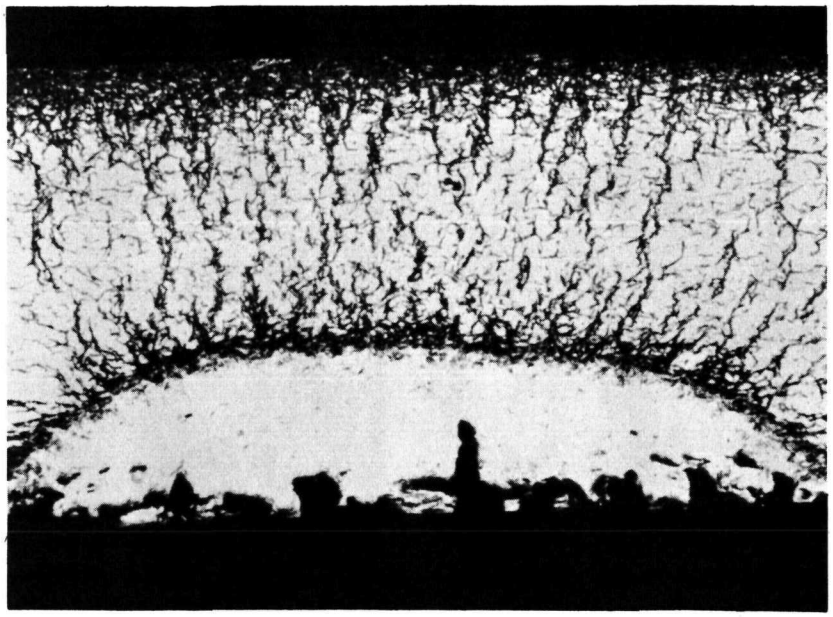

Fig. 27 Extreme local hydriding on inner surface.

Reference Met Y-10-A2 100 X

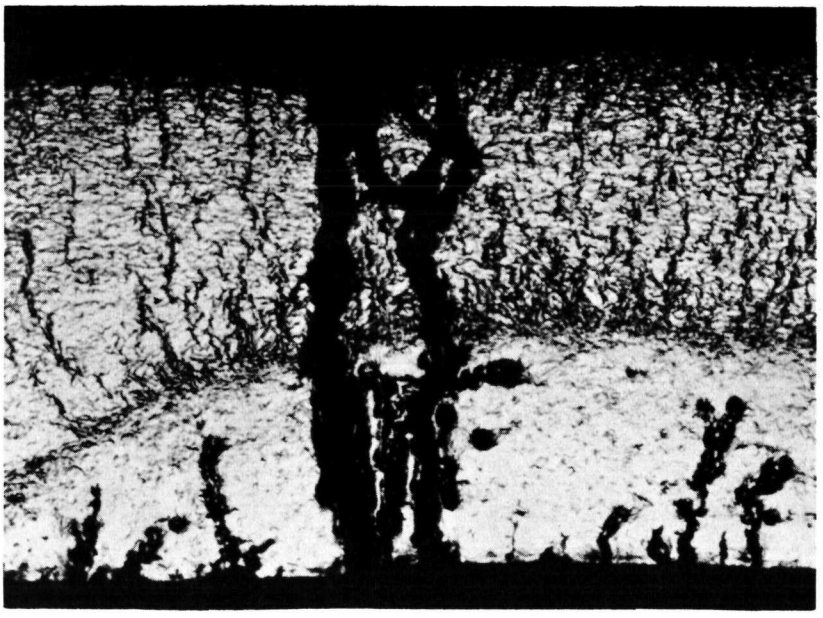

Fig. 28 Same section as figure 13, ground back into the crack.

Reference Met Y-10-A1 100 X

Wire Wrap

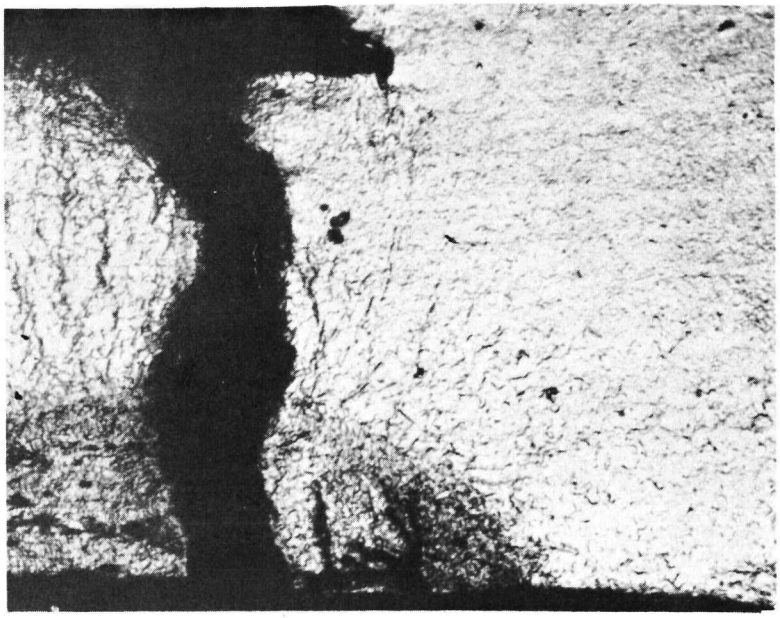

Sheath

Fig. 29 Crack in sheath near wire wrap weld. Same section as in figure 28, ground down to failure.

Reference Met Y-10-A7 100 X

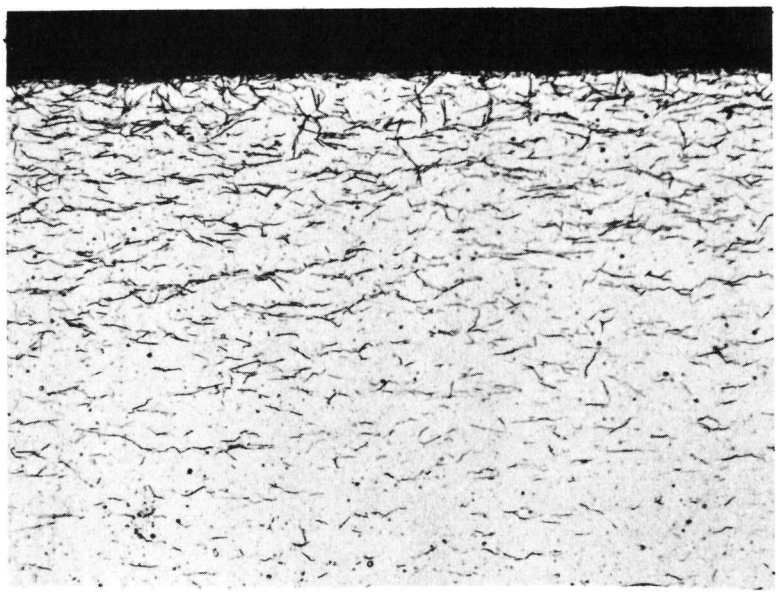

Fig. 30 Hydride concentration in outer surface in region where no localized attack had occurred on the inner surface.

Reference Met Y-10-C1 200 X

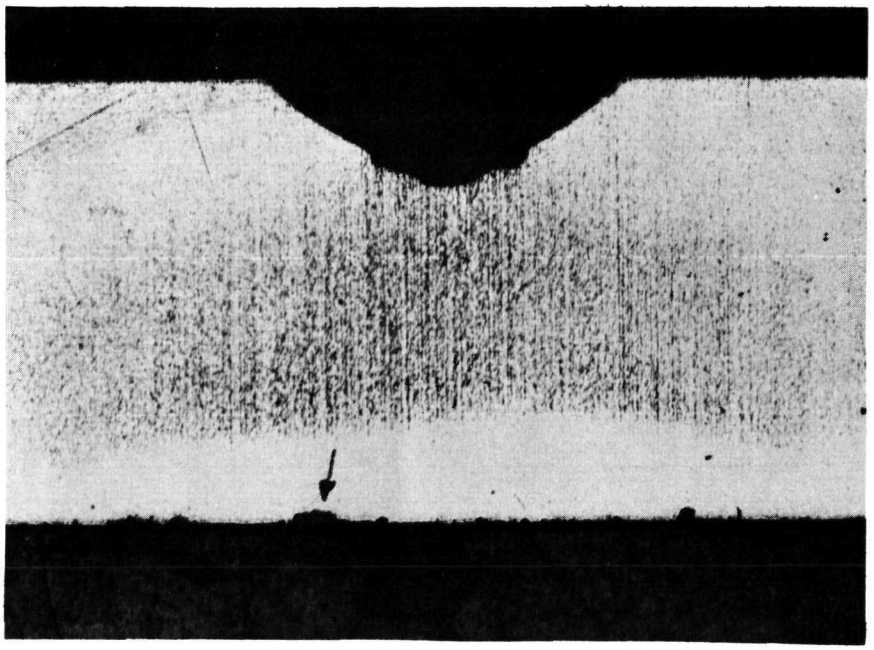

Fig. 31 (a) Longitudinal section through lower end cap. Shows heavy hydriding, dark, and some localized corrosion at UO_2/Zircaloy interface.

Reference Met Y-19-B1 7.5 X

Fig. 31 (b) Localized corrosion at UO_2/Zircaloy interface. Lower end cap.

Reference Met Y-19-B8 100 X

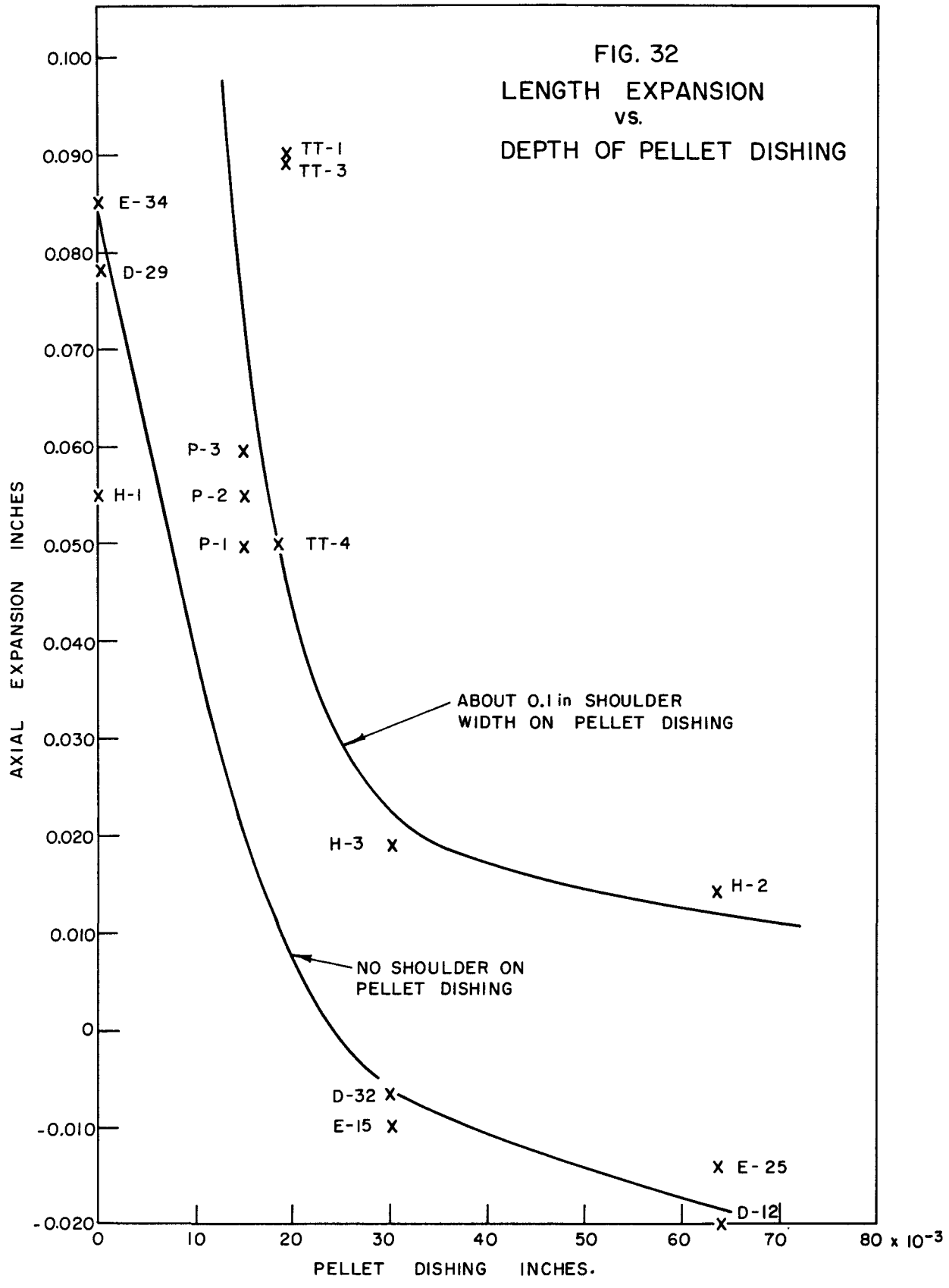
FIG. 32
LENGTH EXPANSION
vs.
DEPTH OF PELLET DISHING
AXIAL EXPANSION INCHES
0.100
0.090
0.080
0.070
0.060
0.050
0.040
0.030
0.020
0.010
0
-0.010
-0.020
TT-1
TT-3
E-34
D-29
H-1
P-3
P-2
P-1
TT-4
ABOUT 0.1 in SHOULDER
WIDTH ON PELLET DISHING
H-3
H-2
NO SHOULDER ON
PELLET DISHING
D-32
E-15
E-25
D-12
0
10
20
30
40
50
60
70
80 x 10-3
PELLET DISHING INCHES.

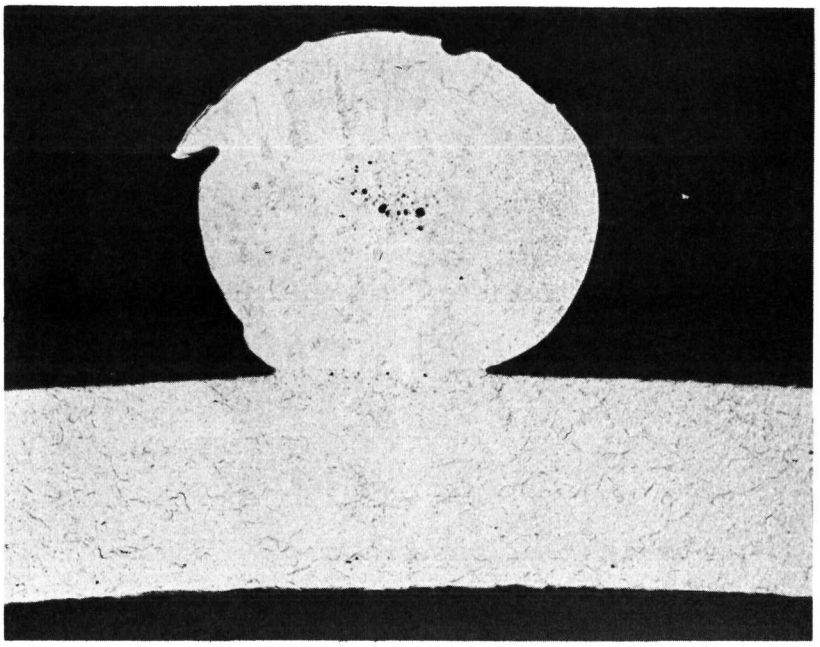

Fig. 33 (a) Archive weld. 50 X

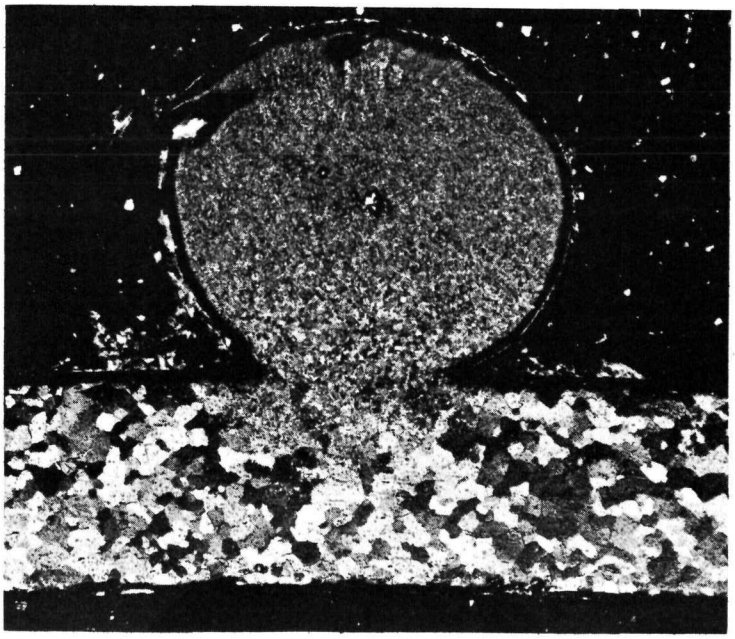

Fig. 33 (b) Archive weld (polarized light) 50 X

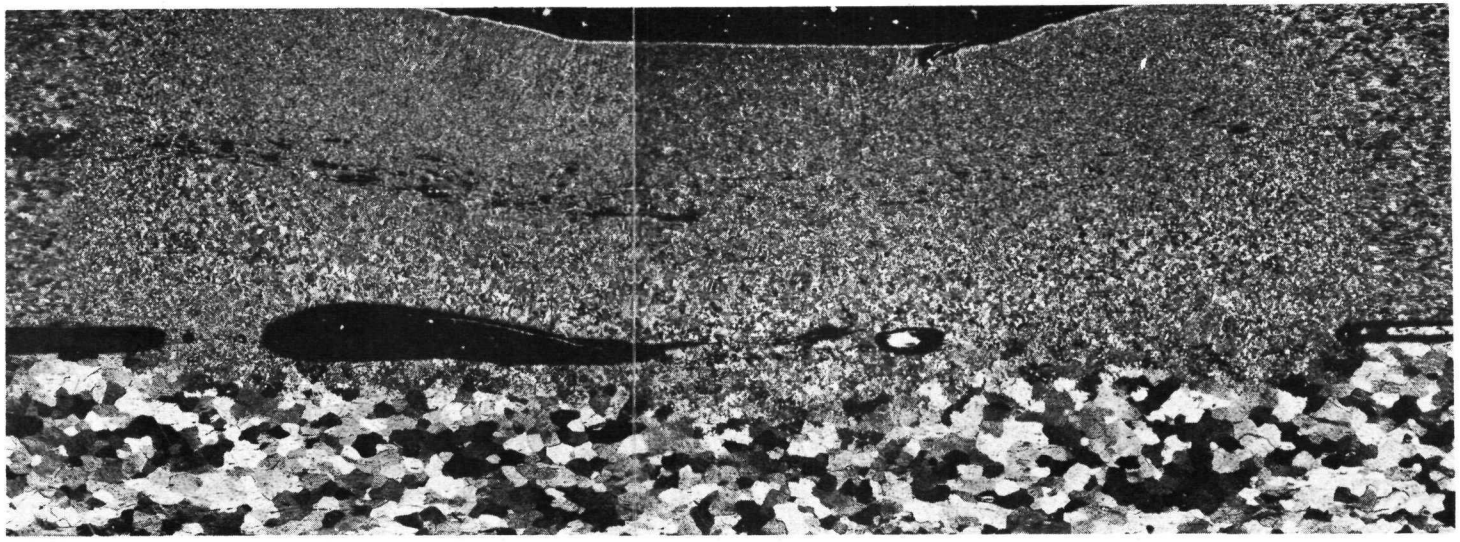

Fig. 34 Archive weld, longitudinal section.

Reference D-378-A2 50 X